University of Twente

EEMCS / Electrical Engineering
Robotics and *Mechatronics*

Modeling and Magnetic-Based Motion Control of a Cluster of Microparticles

F. (Frank) van den Brink

BSc Report

Committee:
Dr. S. Misra
Dr. I.S.M. Khalil
Dr.ir. L. Abelmann
Dr.ir. J. Flokstra

January 2013

Report nr. 001RAM2013
Robotics and Mechatronics
EE-Math-CS
University of Twente
P.O. Box 217
7500 AE Enschede
The Netherlands

Introduction

This bachelor thesis focuses on the modeling and control of a cluster of micro particles. The cluster of micro particles is used to perform point-to-point motion control experiments with and without micro-objects. Further, the cluster of micro particles is used to investigate the feasibility of using micro particles for wireless micro assembly applications. In this bachelor thesis, the following tasks are completed:

1. Investigation of the optimal cluster size within the work space of our magnetic system. This investigation was done by pulling several cluster sizes under a constant magnetic field gradient and comparing their velocities
2. Modeling of a cluster of micro particles. This modeling includes calculation of the contours of the clusters of micro particles
3. Design of micro-objects and a target structure
4. Investigation of the feasibility of using a cluster of micro particles to accomplish wireless micro assembly.

These tasks are explained in the remainder of this thesis. The magnetic system and the control software used to perform the motion control experiments were already developed before this assignment started [15], [17], [28].

Contributions

The results of this thesis contributed to the following paper:

I. S. M. Khalil, F. van den Brink, O. S Sukas, L. Abelmann, and S. Misra, "Microassembly using a cluster of microparticles," in *Proceedings of the IEEE International Conference on Robotics and Automation (ICRA)*, Karlsruhe, Germany, May 2013, *In Press.*

This paper uses the point-to-point motion control and the optimal cluster size results from this thesis. The point-to-point results include motion control of a cluster of micro particles with and without micro-objects. Furthermore, the micro assembly result from this thesis is used in the aforementioned paper.

Modeling and Magnetic-Based Motion Control of a Cluster of Micro Particles

Frank van den Brink, Islam S. M. Khalil and Sarthak Misra
University of Twente, The Netherlands

Abstract— **We investigate a dynamic model for a cluster of micro particles inside a fluid under the influence of magnetic fields. The drag force of a cluster of micro particles is modeled by estimating its geometry using an ellipsoid with an axis ratio of 8. Point-to-point motion control experiments with a cluster of micro particles are carried out with a maximum average velocity of 327 μm/s, and maximum position tracking error of 110 μm/s. Our magnetic system has a workspace of 1.8 mm $\times$ 2.4 mm, and is capable of generating magnetic field and gradient of the magnetic field squared of 5 mT and 0.4 T^2/m, respectively. In order to investigate the feasibility of performing micro assembly tasks using micro particles, a cluster of micro particles is utilized to perform micro manipulation of micro-objects and direct these micro-objects into destinations within a target structure. Micro manipulation experiments are executed with a maximum average velocity and maximum position tracking error of 297 μm/s and 150 μm respectively. Micro assembly of micro objects using a cluster of micro particles is demonstrated at an average velocity of 193 μm/s and an execution time of 18 s.**

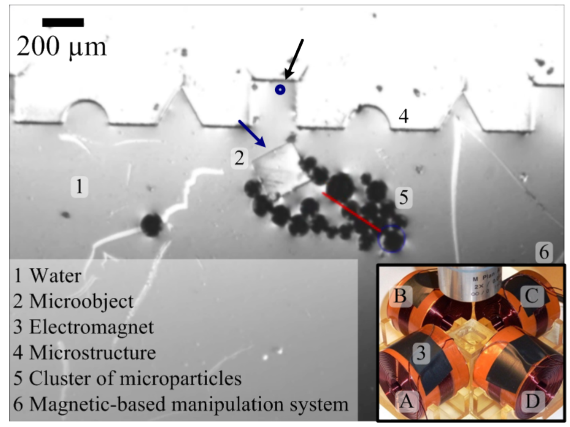

Fig. 1. Magnetic-based micro assembly operation: the cluster of micro particles (5) pushes the micro object (blue arrow) into the micro structure (4) by moving towards a given reference position (black arrow). The external magnetic fields are generated by 4 orthogonal electromagnets, as shown in the inset. The electromagnets surround a fluid reservoir which contains the cluster of micro particles, the micro-object and the target structure. The blue circle and the red line are assigned by our feature tracking software [28]. They represent the position and the velocity of the cluster, respectively.

I. INTRODUCTION

Motivated by the continuous demand for miniaturization in modern technology [1], new micro assembly and micro manipulation techniques have been developed [2]-[7]. Magnetic systems are utilized to control micro particles and magnetotactic bacteria. Applications of these controlled micro particles and bacteria are in the field of minimally invasive surgery (MIS) [8] and micro assembly [9]. Micro assembly using a swarm of magnetotactic bacteria is achieved by Martel *et al.* [10]. A swarm of approximately 5000 bacteria constructed a miniature step pyramid in $\sim$15 minutes. Assembly by microrobots is realized by Fatikow *et al.* [11], [12]. These micro robots are 50 mm to 80 mm in length, and achieve a resolution down to 10 nm and velocities up to 30 mm/s. In the field of MIS, electromagnetic systems have been used to control micro particles [8]. These micro particles can perform targeted drug delivery [13]. Electromagnetic systems can steer the micro particles to hard-to-reach regions within the human body. Utilization of micro particles as drug carriers could reduce negative side effects as the drug can be delivered locally without affecting the healthy tissue [13]. The magnetic force applied on a micro particle depends on its size. Therefore, each micro particle experiences a magnetic force in the range of few nanoNewton to tens of nanoNewton. In this thesis, we focus on utilizing micro particles for micro assembly. We use a cluster of micro particles to increase the magnetic force with a factor of approximately 20. The cluster of micro particles is used to push and/or pull micro objects towards selected destinations within a target structure (Fig. 1). This is done to investigate the feasibility of employing a cluster of micro particles to perform wireless magnetic-based micro assembly. The following tasks are carried out:

1) Investigation of the optimal cluster size within the workspace of our magnetic system
2) Modeling of the cluster of micro particles
3) Design of the motion control system
4) Point-to-point motion control experiments of the cluster of micro particles
5) Investigation of the feasibility of utilizing a cluster of micro particles to accomplish wireless micro assembly.

The remainder of this thesis is organized as follows: Section II discusses the magnetic force modeling, realization of the field-current map, and the design of the closed loop control system. In Section III, the design and manufacturing of the micro-objects and target structure are discussed. Section III also provides descriptions of our magnetic system. The experimental results are provided in Section IV, this Section provides point-to-point motion control results, micro manipulation results and a micro assembly demonstration. Section V provides a discussion. Finally, Section VI concludes and provides directions for future work.

II. MODELING AND CONTROL

A cluster of micro particles experiences a magnetic force and torque under an applied magnetic field. The magnetic force and torque must overcome the drag force and torque to allow the cluster to move inside a fluid. In this section, we discuss the modeling of the drag force and torque and the magnetic force and torque. In addition motion control of a cluster of micro particles is addressed.

A. Magnetic Force Modeling

The magnetic force $\mathbf{F}(\mathbf{P}) \in \mathbb{R}^{3\times1}$ on a micro particle is given by [14]

$$\mathbf{F}(\mathbf{P}) = \nabla(\mathbf{m}(\mathbf{P}) \cdot \mathbf{B}(\mathbf{P})), \tag{1}$$

where $\mathbf{m}(\mathbf{P}) \in \mathbb{R}^{3\times1}$ is the permanent or induced magnetic dipole moment of the micro particle and $\mathbf{B}(\mathbf{P}) \in \mathbb{R}^{3\times1}$ is the induced magnetic field at point ($\mathbf{P} \in \mathbb{R}^{3\times1}$). The permanent or induced magnetic dipole moment is

$$\mathbf{m}(\mathbf{P}) = \alpha_{\mathrm{p}} V_{\mathrm{p}} \mathbf{B}(\mathbf{P}), \tag{2}$$

where V_p is the volume of the micro particle, and α_{p} is a magnetic constant, and is given by

$$\alpha_{\mathrm{p}} = \frac{\chi_m}{\mu}, \tag{3}$$

where χ_m is the magnetic susceptibility constant and μ is the permeability coefficient, and is given by

$$\mu = \mu_0(1 + \chi_m). \tag{4}$$

In our magnetic system, α_{p}=185 kA^2 N^{-1} [15]. Substituting (2) in (1) yields

$$\mathbf{F}(\mathbf{P}) = \alpha_{\mathrm{p}} \frac{4}{3} \pi r_{\mathrm{p}}^3 \nabla(\mathbf{B}^{\mathrm{T}}(\mathbf{P})\mathbf{B}(\mathbf{P})), \tag{5}$$

where r_p is the radius of a micro particle. We assume that the magnetic force on a cluster of micro particles is the sum of the magnetic force on the ith micro particle

$$\mathbf{F}_{\mathrm{c}}(\mathbf{P}) = \sum_{i=1}^{n} \mathbf{F}_i(\mathbf{P}), \tag{6}$$

where n is the number of micro particles within the cluster, and $\mathbf{F}_i(\mathbf{P})$ is the force experienced by the ith micro particle. The magnetic torque on a micro particle is zero, therefore we can not assume that the magnetic torque on a cluster of micro particles is the sum of the magnetic torque on the ith micro particle. The magnetic torque experienced by the cluster of micro particles is given by

$$\mathbf{T}(\mathbf{P}) = \mathbf{m}_{\mathrm{c}}(\mathbf{P}) \times \mathbf{B}(\mathbf{P}), \tag{7}$$

where $\mathbf{T}(\mathbf{P}) \in \mathbb{R}^{3\times1}$ is the magnetic torque and $\mathbf{m}_{\mathrm{c}}(\mathbf{P}) \in \mathbb{R}^{3\times1}$ is the permanent or induced magnetic dipole moment of the cluster.

The magnetic force should overcome the drag force to move the cluster of micro particles. In order to calculate the drag force, it is important to know whether the micro particles move in a low Reynolds number regime. Reynolds number is the ratio between inertial forces and viscous drag forces. Laminar flow for a single micro particle can be assumed when the Reynolds number of the micro particle is less than 0.1. The Reynolds number of a micro particle is given by [15]

$$R_e = \frac{2\rho_{\mathrm{f}} v r_{\mathrm{p}}}{\eta}, \tag{8}$$

where v, η and ρ_f are the micro particle velocity, fluid dynamic viscosity (1 $\mathrm{mPa.s}$) and density (998.2 $\mathrm{kg/m^3}$), respectively. At a linear velocity of 500 μm/s, the Reynolds number is 0.0498. Therefore, laminar flow can be assumed and Stokes' law can be applied for the drag force

$$\mathbf{F}_{\mathrm{d}}(\dot{\mathbf{P}}) = 6\pi\eta r_{\mathrm{p}} \dot{\mathbf{P}}, \tag{9}$$

where $\mathbf{F}_{\mathrm{d}}(\dot{\mathbf{P}}) \in \mathbb{R}^{3\times1}$ is the drag force on a micro particle. A cluster of micro particles experiences a drag force given by

$$\mathbf{F}_{\mathrm{dc}}(\dot{\mathbf{P}}) = \mathcal{F}_{\mathrm{c}} \eta \dot{\mathbf{P}}, \tag{10}$$

where $\mathbf{F}_{\mathrm{dc}}(\dot{\mathbf{P}}) \in \mathbb{R}^{3\times1}$ is the drag force on the cluster, and $\mathcal{F}_{\mathrm{c}}$ is the shape factor for drag of the cluster. This shape factor $\mathcal{F}_{\mathrm{c}}$ is based on the geometry, area and size of the cluster. For micro assembly applications, a micro-object has to be steered towards a targetstructure. The drag force of the micro-object is given by

$$\mathbf{F}_{\mathrm{do}}(\dot{\mathbf{P}}) = \mathcal{F}_{\mathrm{o}} \eta \dot{\mathbf{P}}, \tag{11}$$

where $\mathbf{F}_{\mathrm{do}}(\dot{\mathbf{P}}) \in \mathbb{R}^{3\times1}$ is the drag force on the micro-object, and $\mathcal{F}_{\mathrm{o}}$ is the shape factor for drag of the micro-object. The drag force of the micro-object depends on its geometry. The size of the micro-objects is small relative to the size of the cluster of micro particles. Therefore the drag force on the micro-object is assumed to be nelligible. We assume that a cluster of micro particles has a similar geometry to a disc, and therefore the shape factor $\mathcal{F}_{\mathrm{c}}$ is estimated by [16]

$$\mathcal{F}_{\mathrm{c}} = \frac{32a}{3}, \tag{12}$$

where a is the radius of the disc. Assuming that the area of the disc is the sum of the area of the micro particles, the radius of the disc is given by

$$a = \sqrt{n}\ r_{\mathrm{p}} \tag{13}$$

Substituting (12) and (13) in (10) yields the following equation for the drag force of a cluster of micro particles:

$$\mathbf{F}_{\mathrm{dc}}(\dot{\mathbf{P}}) = \frac{32\sqrt{n}\ r_{\mathrm{p}}}{3} \eta \dot{\mathbf{P}}. \tag{14}$$

The drag torque is given by

$$\mathbf{T}_{\mathrm{d}}(\omega) = \alpha\omega, \tag{15}$$

where ω is the angular velocity of the cluster and α is the rotational drag coefficient. The Reynolds number for a cluster

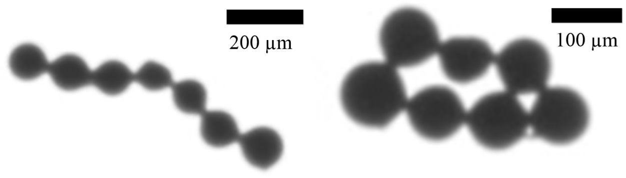

(a) (b)

Fig. 2. The effect of an external magnetic field of 4 mT on the shape of a cluster of micro particles. (a) The shape of a cluster of micro particles in the absence of a magnetic field. In this case, the micro particles are not magnetized and adhesive forces dominate. (b) The shape of the same cluster of micro particles after the application of a magnetic field. In this case the micro particles are magnetized and magnetic forces dominate, and a cluster is formed.

of micro particles is estimated by (8), (9) and (14). Rewriting (8) yields

$$R_e = \Omega_{\mathrm{p}} \frac{\rho_{\mathrm{f}} v}{\eta}, \tag{16}$$

where Ω_{p} is the shape factor for Reynolds number of the micro particle and is given by $\Omega_{\mathrm{p}} = 2r_{\mathrm{p}}$. The Reynolds number for a cluster of micro particles is given by:

$$R_{\mathrm{ec}} = \Omega_{\mathrm{c}} \frac{\rho_{\mathrm{f}} v}{\eta}, \tag{17}$$

where Ω_{c} is the shape factor for Reynolds number of the cluster of micro particles. Rewriting (9)

$$\mathbf{F}_{\mathrm{d}}(\dot{\mathbf{P}}) = \digamma_{\mathrm{p}} \eta \dot{\mathbf{P}}, \tag{18}$$

where $\digamma_{\mathrm{p}}$ is the shape factor for drag of a micro particle. The shape factor for Reynolds number of a cluster of micro particles is estimated by calculating the ratio between the shape factor for drag and the shape factor for Reynolds number. We calculate this ratio for a single micro particle and equate it to the ratio for a cluster of micro particles

$$\frac{\digamma_{\mathrm{p}}}{\Omega_{\mathrm{p}}} = \frac{\digamma_{\mathrm{c}}}{\Omega_{\mathrm{c}}}. \tag{19}$$

Using (12) and (19) yields

$$\Omega_{\mathrm{c}} = \frac{32\sqrt{n} r_{\mathrm{p}}}{9\pi}, \tag{20}$$

which gives the following Reynolds number for a cluster of micro particles

$$R_{\mathrm{ec}} = \frac{32\sqrt{n} r_{\mathrm{p}} \rho_{\mathrm{f}} v}{9\pi\eta}. \tag{21}$$

Inertial forces have to be included in the equation of motion when the Reynolds number of the cluster is larger than 0.1. We observe that the shape of a cluster of micro particles varies with the magnetic field. Therefore the shape factor for drag $\digamma_{\mathrm{c}}$ and the shape factor for Reynolds number Ω_{c} are not constant. In the absence of a magnetic field, the micro particles have negligible magnetization since they are paramagnetic. Adhesive forces between the micro particles dominate. After the application of a magnetic field, the micro particles become magnetic and hence, magnetic forces dominate their behavior. Figs. 2(a) and (b) show the shape of a cluster of micro particles in the absence and presence of a magnetic field, respectively. Due to the change in shape of the cluster of micro particles, the drag force and Reynolds number vary. Compensation of the drag force will be explained in Section II-E.

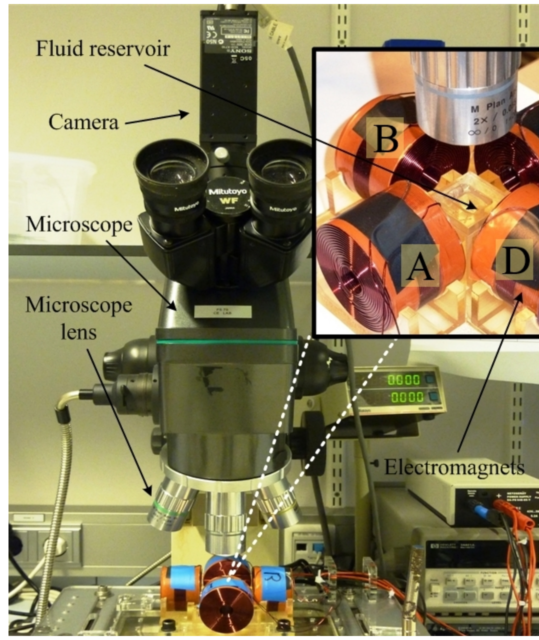

Fig. 3. Magnetic system for the manipulation of micro particles and assembly of micro-objects. The magnetic system consists of four orthogonal electromagnets with a microscope and a vision system [28]. The inset shows the four electromagnets surrounding a fluid reservoir filled with water. The letters A, B, C and D represent the electromagnets.

B. Field Current Map

In order to represent the magnetic field as a function of the currents, a field-current map is realized. The relation between the current through an electromagnet and the magnetic field produced by this electromagnet is linear [7], [17]. Therefore, the magnetic field of the eth electromagnet can be written as

$$\mathbf{B}_e(\mathbf{P}) = \widetilde{\mathbf{B}}_e(\mathbf{P}) i_e, \tag{22}$$

where $\widetilde{\mathbf{B}}_e(\mathbf{P}) \in \mathbb{R}^{3\times m}$ is the magnetic field map and m is the number of electromagnets. The map $\widetilde{\mathbf{B}}_e(\mathbf{P})$ is defined at each point $(\mathbf{P})$ of the workspace of our magnetic system (Fig. 3). $\widetilde{\mathbf{B}}_e(\mathbf{P})$ can be determined by measuring the magnetic field $\big(\mathbf{B}_e(\mathbf{P})\big)$ at each point within the workspace of our magnetic system. We divide the measured magnetic field $\big(\mathbf{B}_e(\mathbf{P})\big)$ by the applied current (i_e) to calculate the magnetic field map $\widetilde{\mathbf{B}}_e(\mathbf{P})$. Due to linearity of our field current map (22), the magnetic field at a point $(\mathbf{P})$ is calculated by the superposition of the contribution of each of the electromagnets

$$\mathbf{B}(\mathbf{P}) = \sum_{e=1}^{m} \mathbf{B}_e(\mathbf{P}) = \sum_{e=1}^{m} \widetilde{\mathbf{B}}_e(\mathbf{P}) i_e. \tag{23}$$

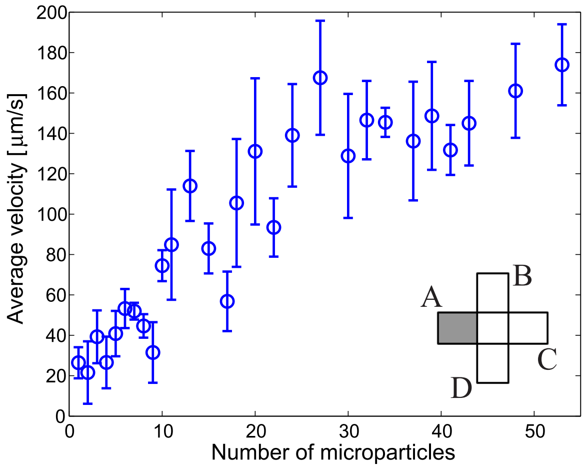

Fig. 4. Average velocity of the cluster of micro particles versus the number of micro particles within the cluster. The average velocity is calculated from 5 motion control experiments. At these motion control experiments, electromagnet A is activated with a current of 0.5 A (darker shade in the inset). The average velocity increases linearly with the number of micro particles up to ∼20 micro particles. The average velocity saturates at 140 μm/s. This allows us to use ∼20 micro particles per cluster in the rest of our experimental work. The letter A, B, C and D represent the electromagnets (Fig. 1). Paramagnetic micro particles with average diameter of 100 μm are used in this experiment (PLAParticles-M-redF-plain from Micromod Partikeltechnologie GmbH, Rostock-Warnemuende, Germany).

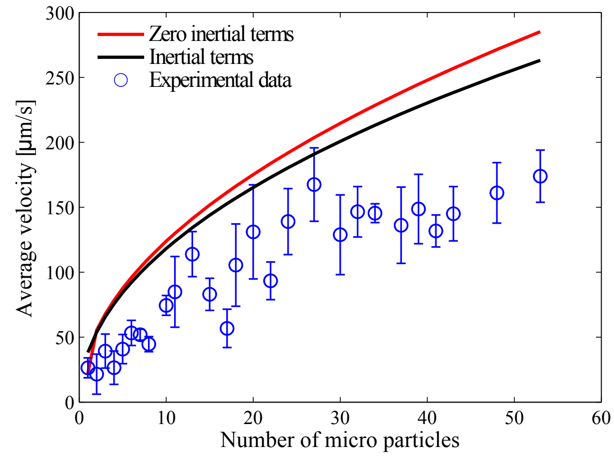

Fig. 5. Comparison between experimental and modeled velocities of the cluster of micro particles in the absence and presence of the inertial term. The magnetic force of the modeled values is based on a magnetic field computed by a finite element model of our magnetic system. In this comparison, (26) is used to compute the magnetic force. The drag force is calculated using (14) assuming that the cluster has a circular geometry. This comparison shows negligible difference when we include the inertial term. Further, we observe a big deviation in the modeled values for cluster sizes larger than 30 micro particles.

Since we control the current through each of the electromagnets rather than the magnetic fields, it is convenient to represent the magnetic force as a function of the currents. Substituting (22) in (5) yields

$$\mathbf{F}(\mathbf{P}) = \alpha_{\mathrm{p}} \frac{4}{3}\pi r_{\mathrm{p}}^3 \nabla\big(\mathbf{I}^{\mathrm{T}}\widetilde{\mathbf{B}}^{\mathrm{T}}(\mathbf{P})\widetilde{\mathbf{B}}(\mathbf{P})\mathbf{I}\big), \tag{24}$$

where $\mathbf{I} \in \mathbb{R}^{4\times m}$ is the current vector. The magnetic force can be controlled by controlling the currents at each electromagnet. We rewrite (22) into (25) to calculate the desired currents for a given magnetic force or field

$$i_e = \widetilde{\mathbf{B}}_e(\mathbf{P})^{\dagger}\mathbf{B}_e(\mathbf{P}), \tag{25}$$

where $\widetilde{\mathbf{B}}_e(\mathbf{P})^{\dagger}$ is the pseudo-inverse of $\mathbf{B}_e(\mathbf{P})$. The magnetic force on the cluster of micro particles depends on the number of micro particles within the cluster (6). Therefore it is important to select the number of micro particles within the cluster.

C. Optimal Cluster Size

In order to develop a control system for the motion of a cluster of micro particles, first the optimal cluster size has to be chosen. This is done by evaluating the velocity of the cluster at different cluster sizes under a constant magnetic field. The result of this experiment is shown in Fig. 4. In this experiment, a current of 0.5 A is applied on electromagnet A. This current generates a gradient of the magnetic field squared of 0.2 T^2/m. Five experiments are conducted for each cluster size. Fig. 4 shows an almost linear increase of the average velocity of the clusters up to ∼20 micro particles. This implies that (6) is a valid assumption. Substituting (24) in (6) yields the following magnetic force on a cluster of micro particles

$$\mathbf{F}_{\mathrm{c}}(\mathbf{P}) = \sum_{i=1}^{n} \alpha_{\mathrm{p}} \frac{4}{3}\pi r_{\mathrm{p}i}^3 \nabla\big(\mathbf{I}^{\mathrm{T}}\widetilde{\mathbf{B}}^{\mathrm{T}}(\mathbf{P})\widetilde{\mathbf{B}}(\mathbf{P})\mathbf{I}\big), \tag{26}$$

where $r_{\mathrm{p}i}$ is the radius of the ith particle in the cluster. We observe a saturation in the velocity for a cluster size of ∼20 micro particles and at average velocity of 140 μm/s. Therefore, a cluster size of ∼20 micro particles is chosen to be the optimal cluster size throughout our experimental work. A larger cluster size would not provide larger net force. However a larger cluster size has more limitations due its size relative to the size of the workspace of 2.4×1.8 mm^2. The asymptotic behavior can be due to the increase of Reynolds number. At higher Reynolds numbers the drag force increases quadratically with the velocity, not linearly. Also the size of the workspace is a reason for the asymptotic behavior of the cluster. Larger cluster sizes reach closer to the edge of the reservoir during motion control experiments, and therefore experience larger meniscus forces.

D. Model Validation and Shape Analysis

Fig. 5 shows a comparison between our model and the experimental values, both with and without the inertial force. In this model, (14) is used for the drag force and (26) is used for the magnetic force. The magnetic force is computed based on a finite element model of our magnetic system. Fig. 5 shows no big deviation between excluding and including the inertial term as we expected with our estimation of the Reynolds number for the cluster of micro particles. The modeled values represent the experimental values up to a cluster size of ∼ 30 micro particles, which is in our working

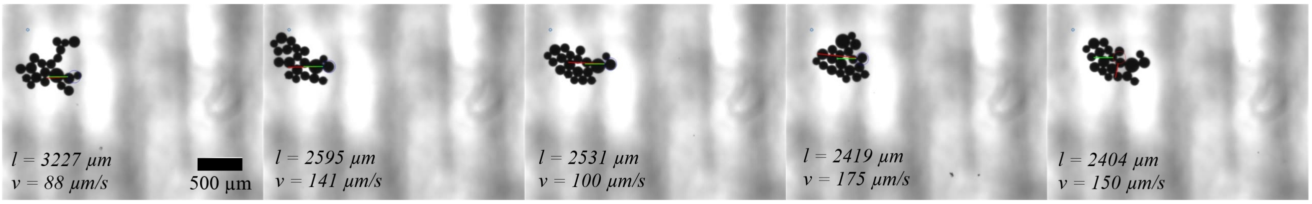

Fig. 6. Demonstration of the dynamic nature of the shape of the cluster of micro particles. The shape of the cluster varies with time and at each experiment. This demonstration shows 5 different shapes for the same cluster of 20 micro particles. The difference in shape explains the deviation in contour and velocity. From left to right, the cluster respectively has a contour length (l) of 3227 μm, 2595 μm, 2531 μm, 2419 μm and 2404 μm and an average velocity (v) of 88 μm/s, 141 μm/s, 100 μm/s, 175 μm/s and 150 μm/s.

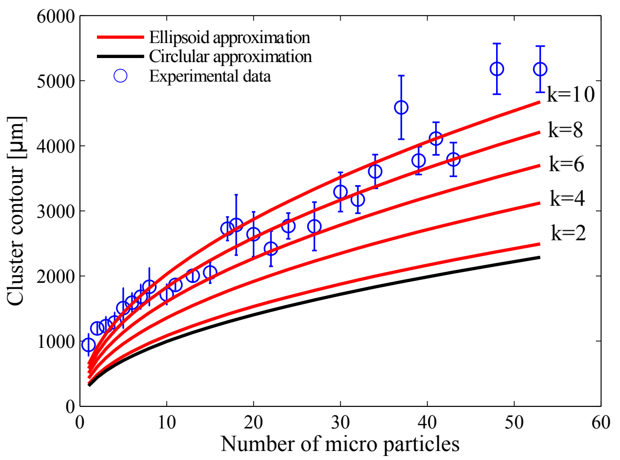

Fig. 7. Comparison between experimental and modeled contours versus the number of micro particles in a cluster. Modeled values are computed by approximating the geometry of the cluster with a circle and ellipsoid with a ratio of 2, 4, 6, 8 and 10. Based on the result of this comparison, an ellipsoid with a ratio of 8 is selected to be the optimum estimation for the geometry of a cluster of micro particles

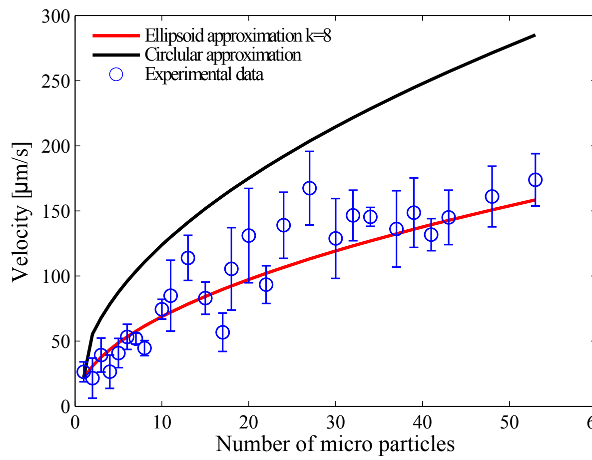

Fig. 8. Comparison between modeled and experimental velocities of the cluster of micro particles. The modeled values are computed by approximating the geometry of the cluster with a circle and an ellipsoid with a ratio between the major and minor axis of 8. For the ellipsoid (28) is used as the equation for drag force. Based on this comparison, we conclude that an ellipsoid with a ratio of 8 is the best approximation to model a cluster of micro particles within our magnetic system

range. At cluster sizes larger than 30 micro particles, the model values show larger deviations. This can be due to the reasons explained in Sec. II-C but also due to the geometry of the cluster. In order to investigate if a circular disc is the best assumption for the geometry of a cluster of micro particles, we analyze the shape of all the clusters used for the experiment of Sec. II-C. We calculate the contours of these clusters and compare these contours with the contours of a circle and ellipsoid with different ratios between the major and minor axis, k=a:b. The process of calculating the contour of a cluster of micro particles is shown in Fig. 11. First the original image (Fig. 11.a) is loaded into MATLAB and then it is converted to a binary image (Fig. 11.b) which makes it possible to compute the perimeter line (Fig. 11.c). The contour of the cluster in units of pixels is obtained by taking the area of the perimeter line since these lines are 1 pixel in width. The images consist of 512 $\times$ 384 pixels which cover a workspace of 2.4 mm $\times$ 1.8 mm which means 4.6875 μm per pixel. The contours of the ellipsoids are estimated using

$$C_{\mathrm{e}} = \pi[3(a+b) - \sqrt{(a+3b)(3a+b)}], \tag{27}$$

where a and b are the major and minor axis lengths of the ellipsoid. Fig. 7 shows the modeled ellipsoid contours, a contour of a circular disc and the contours of the clusters of micro particles with the number of micro particles in a cluster. Based on Fig. 7, we select an ellipsoid with ratio of k=8, to represent the geometry of a cluster of micro particles. The deviations in cluster contour of the experimental values are due to the varying geometrie of a cluster. Fig. 6 shows an example of the different geometries and contours a cluster of 20 micro particles can have.

The viscous drag coefficient of a randomly moving ellipsoid is given by [16]

$$\digamma_{\mathrm{e}} = \frac{6\pi\eta a}{\ln\left(\frac{2a}{b}\right)}, \tag{28}$$

which yields a drag force:

$$\mathbf{F}_{\mathrm{de}}(\dot{\mathbf{P}}) = \frac{6\pi\eta a}{\ln\left(\frac{2a}{b}\right)}\dot{\mathbf{P}}. \tag{29}$$

This equation is only valid for $a^2 >> b^2$. Fig 8 shows the velocities of the cluster, circular disc and ellipsoid disc with ratio of k=8. We observe that the drag force of an ellipsoid

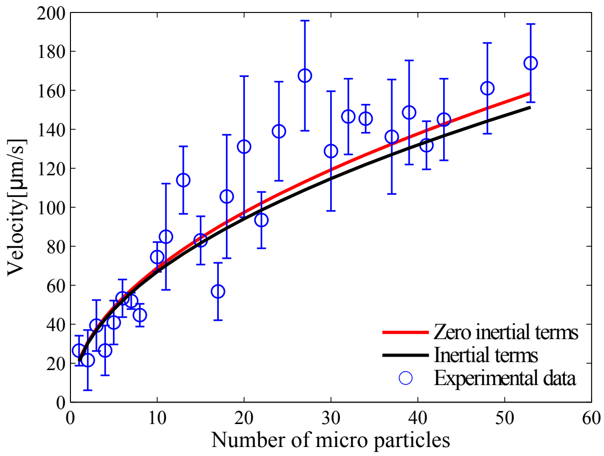

Fig. 9. Experimental and modeled velocities of the cluster of micro particles in absence and presence of the inertial term. The modeled velocities are computed by approximating the geometry of the cluster to be an ellipsoid with a ratio between the major and minor axis of 8. The result of this comparison allows us to neglect the inertial term in the equation of motion.

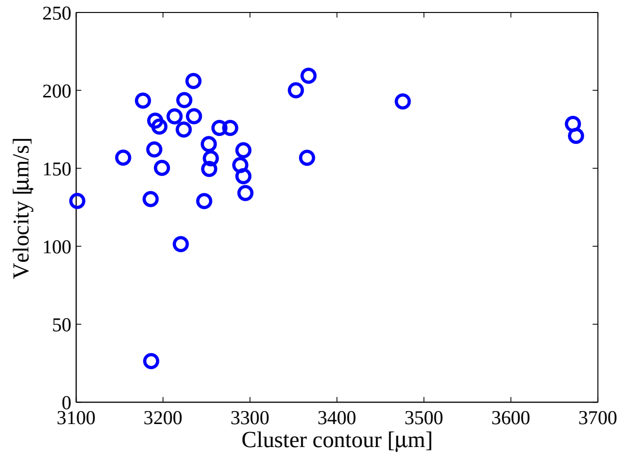

Fig. 10. Relation between the contour and the velocity of a cluster of micro particles. These results are based on 30 velocity experiments with a cluster of 20 micro particles. During these experiments the cluster of micro particles is pulled from the middle to the edge of the workspace under influence of a gradient of the magnetic field squared of 0.2 T^2/m. We conclude from this figure that there is no clear relation between the contour of a cluster and the velocity of the cluster.

is a better representation of a cluster of micro particles in our magnetic system than a circle. Therefore, we use (29) to model the drag force in our magnetic system.

Our estimation for the Reynolds number of a cluster of micro particles (21) is based on a circular geometry. Therefore we made a comparison between including and excluding the inertial term for an ellipsoid-shaped cluster of micro particles. Fig. 9 shows our model with and without the inertial term. Based on Fig. 9, we conclude that the inertial term can be neglected.

A cluster of micro particles never occurs with equal geometry (hence the contour deviations in Fig. 7). Fig. 6 shows an example of the different shapes of a cluster of 20 micro particles. In order to investigate if there is a relation between the shape of a cluster of micro particles and its drag force, 30 velocity experiments with a cluster of 20 micro particles are done. In these experiments the cluster of micro particles moves from the middle of the workspace to the edge under a gradient of the magnetic field squared of 0.2 T^2/m. Fig. 10 shows a comparison of the different contours and velocities of these experiments. From these experiments, we conclude that there is no clear relation between the contour of a cluster of micro particles and its drag force.

E. Closed-Loop Control

We conclude from Fig. 9 that the inertial force can be neglected, and therefore the following equation of motion for a cluster of micro particles holds:

$$\mathbf{F}(\mathbf{P}) - \mathbf{F}_{\mathrm{de}}(\dot{\mathbf{P}}) = 0. \tag{30}$$

In order to allow the cluster to follow any reference position ($\mathbf{P}_{\mathrm{ref}}$) within the workspace of the magnetic system, the following magnetic force is devised:

$$\mathbf{F}(\mathbf{P}) = \mathbf{F}_{\mathrm{de}}(\dot{\mathbf{P}}) - \mathrm{M}_{\mathrm{n}}\left(\mathbf{K}_{\mathbf{d}}\dot{\mathbf{e}} + \mathbf{K}_{\mathbf{p}}\mathbf{e}\right), \tag{31}$$

where M_{n} is the nominal mass of the cluster and $\mathbf{K}_{\mathbf{p}}$ and $\mathbf{K}_{\mathbf{d}}$ are the controller positive-definite gain matrices, and are given by

$$\mathbf{K}_{\mathbf{p}} = \begin{bmatrix} k_{\mathrm{p1}} & 0 \\ 0 & k_{\mathrm{p2}} \end{bmatrix} \text{ and } \mathbf{K}_{\mathbf{d}} = \begin{bmatrix} k_{\mathrm{d1}} & 0 \\ 0 & k_{\mathrm{d2}} \end{bmatrix}, \tag{32}$$

where $k_{\mathrm{p}i}$ and $k_{\mathrm{d}i}$, for $(i = 1, 2)$, are the proportional and derivative gains, respectively. The drag force in (31) only models the drag of the cluster of micro particles. An extra drag force term has to be included, when performing motion control of a micro-object. The total drag force is estimated by a drag force observer (Fig. 12). From this drag force observer we estimate a drag force:

$$\widehat{\mathbf{F}}_{\mathrm{d}}(\dot{\mathbf{P}}) \triangleq \widehat{\mathbf{F}}_{\mathrm{dc}}(\dot{\mathbf{P}}) + \widehat{\mathbf{F}}_{\mathrm{do}}(\dot{\mathbf{P}}), \tag{33}$$

where $\widehat{\mathbf{F}}_{\mathrm{dc}}(\dot{\mathbf{P}})$ and $\widehat{\mathbf{F}}_{\mathrm{do}}(\dot{\mathbf{P}})$ are the observed drag force on the cluster and on a micro object, respectively. Using the drag force observer, the following magnetic force is computed:

$$\mathbf{F}(\mathbf{P}) = \widehat{\mathbf{F}}_{\mathrm{d}}(\dot{\mathbf{P}}) - \mathrm{M}_{\mathrm{n}}\left(\mathbf{K}_{\mathbf{d}}\dot{\mathbf{e}} + \mathbf{K}_{\mathbf{p}}\mathbf{e}\right). \tag{34}$$

The estimated drag force $\widehat{\mathbf{F}}_{\mathrm{d}}(\dot{\mathbf{P}})$ is calculated using the drag force observer (Fig. 12) [17]:

$$\widehat{\mathbf{F}}_{\mathrm{d}}(\mathbf{P}) = \frac{g}{s+g}\left[\mathbf{F}(\mathbf{P}) - g\mathrm{M}_{\mathrm{n}}\dot{\mathbf{P}}\right] - g\mathrm{M}_{\mathrm{n}}\dot{\mathbf{P}}, \tag{35}$$

where g is a positive gain of the low-pass filter of the drag force observer (Fig.12). The position ($\mathbf{e}$) and velocity ($\dot{\mathbf{e}}$) tracking errors of the cluster are given by

$$\mathbf{e} = \mathbf{P}_{\mathrm{ref}} - \mathbf{P} \text{ and } \dot{\mathbf{e}} = \dot{\mathbf{P}}_{\mathrm{ref}} - \dot{\mathbf{P}}, \tag{36}$$

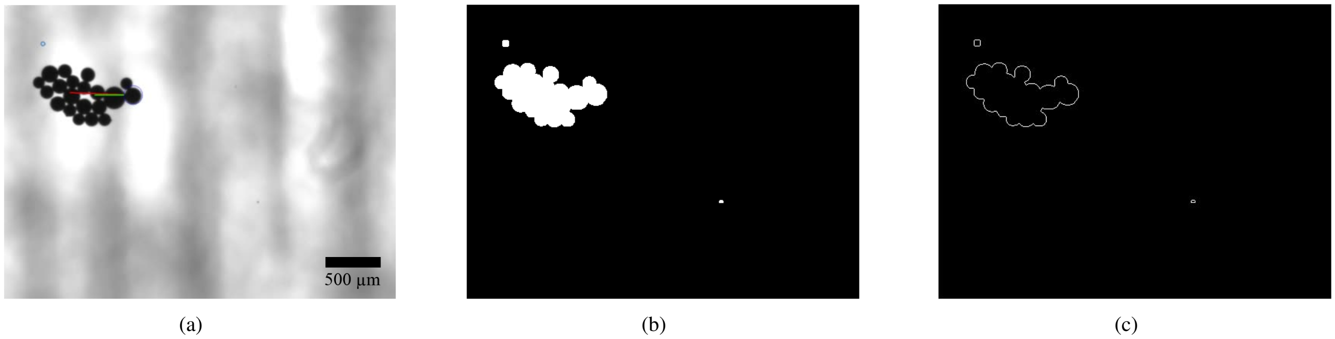

Fig. 11. Computation of the contour of a cluster of micro particles using image processing. (a) The original image. (b) The binary image. (c) Perimeter line obtained from the binary image. In order to calculate the contour of a cluster of micro particles, the original image first is converted to a binary image and then processed to a perimeter line. The perimeter line is 1 pixel in width. Therefore, the contour of the cluster can be calculated by taking the area of the perimeter line.

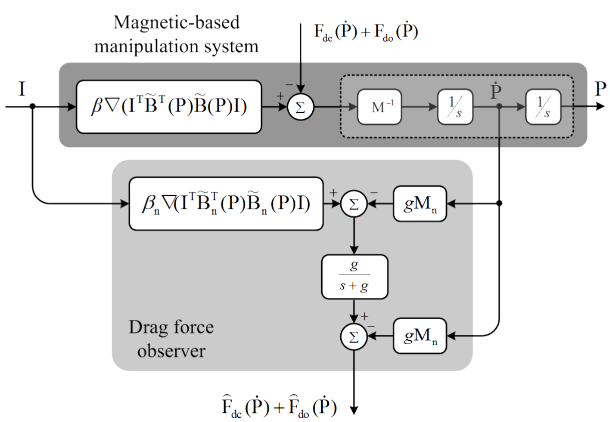

Fig. 12. Drag force observer [17]: The drag forces on the cluster of micro particles ($\widehat{\mathbf{F}}_{\mathrm{dc}}(\dot{\mathbf{P}})$) and the micro-object ($\widehat{\mathbf{F}}_{\mathrm{do}}(\dot{\mathbf{P}})$) are estimated using the applied current ($\mathbf{I}$) to each of the electromagnets, and the velocity ($\dot{\mathbf{P}}$) of the cluster. The estimated drag forces ($\widehat{\mathbf{F}}_{\mathrm{dc}}(\dot{\mathbf{P}})$ and $\widehat{\mathbf{F}}_{\mathrm{do}}(\dot{\mathbf{P}})$) are used by the control law (34) to compensate for the drag forces. M and $\mathrm{M_n}$ are the mass of the cluster and its nominal value, respectively. g is the positive gain of the low-pass filter associated with the drag force observer. β is a magnetic constant given by $\alpha_{\mathrm{p}}\frac{4}{3}\pi r_{\mathrm{p}}^3$, and β_n represents its nominal value.

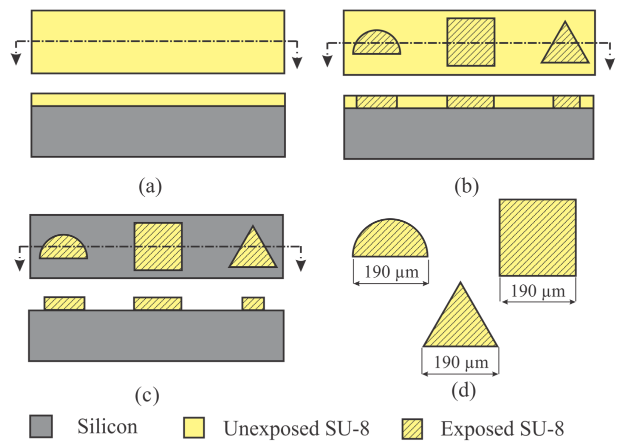

Fig. 13. Fabrication of the micro-objects: (a) Spin coating of SU-8 (MicroChem Corp., Newton, USA) on a silicon wafer. (b) Transferring the patterns of the micro-objects to the SU-8 layer after pre-bake and ultraviolet-exposure. (c) Realization of the micro-objects after post-exposure bake and developing the unexposed SU-8 layer. (d) Release of the micro-objects by etching the silicon wafer.

where $\mathbf{P}_{\mathrm{ref}}$ and $\dot{\mathbf{P}}_{\mathrm{ref}}$ are the reference position and velocity, respectively. Substitution of the desired magnetic force (31) in (30) yields the following tracking error dynamics:

$$\mathbf{K_d}\dot{\mathbf{e}} + \mathbf{K_p}\mathbf{e} = 0. \tag{37}$$

This means that the tracking error ($\mathbf{e}$) is stable if and only if $\mathbf{K_d}^{-1}\mathbf{K_p} > 0$. Therefore, the desired magnetic force allows the cluster to follow the given reference position, while simultaneously compensating for the drag forces on the cluster and the micro-object.

III. EXPERIMENTAL SETUP

All experiments are conducted on a magnetic system consisting of a fluid reservoir, 4 electromagnets and a microscope with camera to provide feedback for the control system. Micro-objects and micro targetstructures to perform micro assembly are made of SU-8-50 and SU-8-100.

A. Magnetic System

The magnetic system (Fig. 3) consists of four orthogonal electromagnets surrounding a fluid reservoir of 11.5 mm $\times$ 11.5 mm. The magnetic system is capable of generating a magnetic field and gradient of the magnetic field squared of 5 mT and 0.4 $\mathrm{T^2/m}$, respectively. A microscopic vision system mounted on top of the electromagnets tracks the motion of the cluster of micro particles. The tracking information is used to realize the control system. Paramagnetic micro particles with average diameter of 100 μm are used (PLAParticles-M-redF-plain from Micromod Partikeltechnologie GmbH, Rostock-Warnemuende, Germany).

B. Micro-objects and Micro-targetstructure

The micro-objects and micro-targetstructure are fabricated using SU-8-50 and SU-8-100 (MicroChem Corp., Newton, USA), which is a commonly used epoxy-based photoresist. This material is selected for its mechanical stability and ease of fabrication. A silicon wafer with thickness and diameter 500 μm and 100 μm and <100> crystal orientation is spin

TABLE I

MANUFACTURING PROCESS PARAMETERS FOR THE MICRO-OBJECTS (SU-8-50) AND TARGETSTRUCTURE (SU-8-100)

Type	Thickness	Spin	Pre-bake		Expose	Post-exposure bake		Develop	Hard bake	
	[μm]	Speed [rpm]	Temp. [°C]	Time [min]	Time [s]	Temp. [°C]	Time [min]	Time [min]	Temp. [°C]	Time [min]
SU-8-50 (micro-objects)	50±8%	3000	95	20	50	80	10	3	120	120
SU-8-100 (targetstructure)	100±8%	3500	95	120	24	75	35	5	120	120

TABLE II

EXPERIMENTAL MOTION CONTROL RESULTS OF THE CLUSTER OF MICRO PARTICLES. THE RESULTS ARE OBTAINED FROM 10 MOTION CONTROL TRIALS

Motion Control Operation	Average Velocity [μm/s]	Maximum Average Velocity [μm/s]	Average Tracking Error [μm]	Maximum Tracking Error [μm]	Execution Time [s]
Point-to-Point Control	193±85	327	37±47	110	-
Micro Manipulation	194±63	297	103±81	150	-
Micro Assembly	193	-	-	-	18 s

coated with a layer of SU-8-50 (Fig. 13 (a)). After pre-baking the wafer, patterns of the micro-objects are transferred to the SU-8 layer by ultraviolet (UV) exposure (Fig. 13 (b)). After that, the wafer is further baked (post-exposure bake). The micro-objects are realized by developing the SU-8 layer in RER600 (ARCH Chemicals)(Fig. 13 (c)). To achieve mechanical stability of the micro-objects, the wafer is hard baked. Now an oxygen plasma treatment is performed on the SU-8 micro-objects for 30 seconds to make them hydrophilic. The micro-objects are released by etching away the silicon wafer in a 5 wt % TMAH solution at 85°C (Fig. 13 (d)). A filter is used to collect the micro-objects.

Fabrication of the micro-targetstructure (Fig. 1) is similar to that of the micro-objects. However, instead of releasing it by etching away the silicon wafer, the silicon wafer is diced into 11 mm^2 pieces which all have a micro structure and fit into the fluid reservoir of the magnetic system.

IV. EXPERIMENTAL RESULTS

The cluster of micro particles is steered towards different reference positions within the workspace of our magnetic system. Furthermore, feasibility of employing a cluster of micro particles for micro assembly applications is investigated. First, point-to-point motion control experiments with a cluster of micro particles are conducted. Second, micro manipulation experiments are done, the cluster is used to direct a micro-object towards different reference positions throughout the workspace. Third, micro assembly experiments are carried out, the cluster is employed to steer the micro-object into a selected destination within a targetstructure. Table II shows the experimental results of the motion control operations. The parameters of this experiments are listed in Table III.

A. Point-to-Point Motion Control

Fig. 14 shows the result of a point-to-point motion control operation of a cluster of micro particles. The average velocity and tracking error of 10 point-to-point motion control experiments are 193±85 μm/s and 37±47 μm. The maximum average velocity and tracking error are 327 μm/s and 110 μm. We observe a large difference of 134 μm/s and 73 μm between the average velocity and tracking error and the maximum average velocity and tracking error. Also there are large deviations in the average velocity and the tracking error, 85 μm/s and 47 μm, respectively. The large deviations in tracking error can be explained by the different reference positions assigned to the clusters. We observed that some locations in the workspace are harder to reach than others. The large deviations in the average velocity can be explained by the anisotropic nature of our magnetic system. The magnetic field of an electromagnet drops faster in the perpendicular direction from the electromagnet than in the parallel direction. Our magnetic system has four electromagnets, therefore the magnetic field drops faster in the diagonal direction than in the horizontal and vertical direction. This causes higher directional magnetic field gradients and therefore faster motion in the diagonal direction compared to the horizontal or vertical direction. We conclude from this experiment that the selected cluster size of $\sim$20

TABLE III

EXPERIMENTAL PARAMETERS AND CONTROLLER GAINS

Parameter	Value	Parameter	Value
r_{p} [μm]	50	n	$\sim$20
$\mathrm{M_n}$ [kg]	7.33×10^{-10}	χ_{m}	0.17 ± 0.007
η [mPa.s]	1	g [rad/s]	30
$k_{\mathrm{p1,p2}}$ [s^{-2}]	10	$k_{\mathrm{d1,d2}}$ [s^{-1}]	20

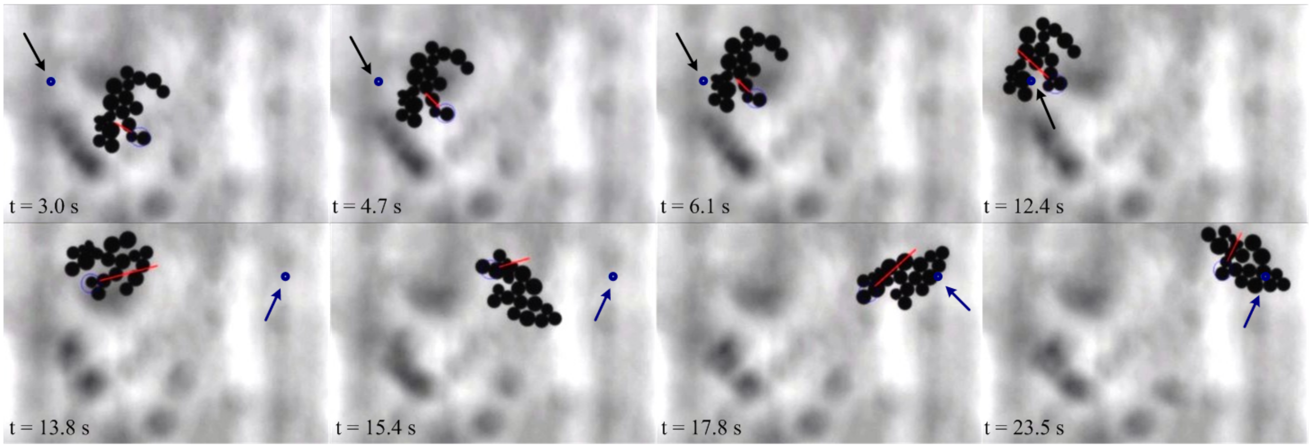

Fig. 14. Motion control of the cluster of micro particles under the influence of the applied magnetic fields at various time (t) instants. The cluster follows two reference positions indicated by the black and blue arrows in the upper and bottom rows, respectively. At this particular experiment the cluster of micro particles follows these reference positions at a velocity of 144 μm/s, and maximum position tracking error of 50 μm. Average velocities and tracking errors of 10 motion control experiments are listed in Table II. This motion control experiment is done using the control law (34). The controller gains are listed in Table III. The cluster consists of 19 micro particles. Paramagnetic micro particles with average diameter of 100 μm are used in this experiment (PLAParticles-M-redF-plain from Micromod Partikeltechnologie GmbH, Rostock-Warnemuende, Germany). The large blue (light) circle is assigned by our feature tracking software [28], whereas the small blue circle indicates the reference position. The red (light) line indicates the velocity vector of the cluster.

micro particles operates in the workspace of our magnetic system and that the magnetic field gradients of the system provide enough magnetic force to overcome the drag force acting on the cluster.

B. *Motion Control of Micro-objects*

In order to investigate the feasibility of using a cluster of micro particles for micro assembly applications, first micro manipulation experiments with micro-objects are executed. A micro-object is pushed or pulled towards a reference position within the workspace of our magnetic system. Fig. 15 shows an example of a micro manipulation experiment. Based on 10 micro manipulation experiments, the average velocity and tracking error are 194$\pm$63 μm/s and 103$\pm$81 μm with a maximum average velocity and tracking error of 297 μm/s and 150 μm (also listed in Table II). From the small difference between the average velocity of the point-to-point motion control experiment of a cluster of micro particles and the average velocity of the micro manipulation experiment, we conclude that (29) also holds for the drag force during micro manipulation experiments. We observe a big tracking error of the micro manipulation experiment. This is because not the micro-object but a micro particle in the cluster is tracked and therefore this micro particle is steered toward the reference position, dragging the micro-object with it. This experiment shows that the cluster of micro particles generates enough force to push or pull a micro-object towards a given reference position.

C. *Micro Assembly Application*

Finally, the cluster of micro particles is employed to perform a micro assembly task. A micro-object is assembled within a targetstructure. Fig.16 shows a micro assembly operation. A triangular micro object is steered towards a specific destination within the targetstructure. First a cluster of micro particles is used to pull the triangular micro-object out of a rectangular destination within the targetstructure. The cluster is then used to push the triangular micro-object into its triangular destination within the targetstructure. After completing its micro assembly task, the cluster moves away from the micro-object. The total micro assembly task is executed with an average velocity of 193 μm/s and an execution time of 18 s. From this experiment we can conclude that micro assembly using a cluster of micro particles is feasible.

V. Discussion

Interaction forces at micro scale limited us to accurately control the cluster of micro particles in the neighbourhood of the target structure. Interaction phenomena at micro scale are a common topic of interest in research to micro manipulation systems [18]. In order to improve micro assembly results in the future, further investigation of interaction forces at micro scale has to be carried out. Also, to get more succesful micro assembly results, adjustments to the targetstructure could be made. A target structure incorporated in the fluid reservoir could solve the problem. Furthermore, we encountered large deviations in postion tracking error and velocity. This is due to the anisotropic nature of our magnetic system. Different directional magnetic field gradients cause different maximum forces for different directions.

VI. CONCLUSIONS AND FUTURE WORK

In this work, a cluster of micro particles is modeled and controlled. The cluster of micro particles is then used to investigate the utilization of micro particles in a micro assembly task. First, the optimal number of micro particles within a cluster in our magnetic system is determined. The selected cluster size is used to carry out point-to-point motion control of a cluster of micro particles at an average velocity of 193$\pm$85μm/s and position tracking error

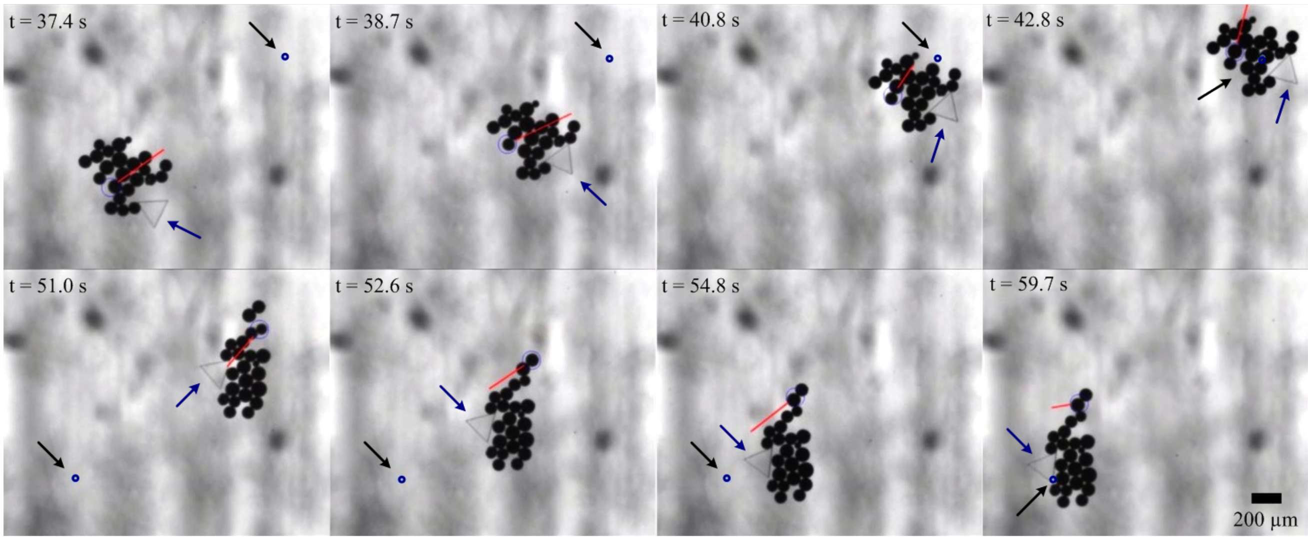

Fig. 15. Micromanipulation of a triangular micro-object towards reference positions using a cluster of micro particles at various time (t) instants. The cluster pushes the micro-object under the influence of the controlled magnetic fields generated by the control law (34). During this micro manipulation experiment, the velocity of the cluster is 204 μm/s, and the maximum position tracking error of 75 μm is accomplished (error between the reference position and the center of mass of the micro-object). Average velocities and tracking errors of 10 motion control experiments are listed in Table II. The controller gains are listed in Table III. The large blue (light) circle is assigned by our feature tracking software [28], whereas the small blue circle indicates the reference position. The red (light) line indicates the velocity vector of the cluster of micro particles. The black arrows indicate the first and second reference positions in the top and bottom rows, respectively. The blue arrows indicate the micro-object. The cluster consists of 23 micro particles. Paramagnetic micro particles with average diameter of 100 μm are used in this experiment (PLAParticles-M-redF-plain from Micromod Partikeltechnologie GmbH, Rostock-Warnemuende, Germany).

of 37$\pm$47μ/s. In order to investigate the utilization of a cluster of micro particles in motion control of micro-objects, micro manipulation experiments are conducted at an average velocity and position tracking error of 194$\pm$63μm/s and 103$\pm$81μm, respectively. Finally, feasibility of employing a cluster of micro particles to perform a micro assembly task is demonstrated. A micro-object is assembled to a selected destination within a target structure at an execution time of 18 s.

Future work includes control of the cluster of micro particles in the three dimensional (3D) space. Further, automation of the micro assembly task will be achieved. In order to realize this automated micro assembly operation the following steps need to be done:

1) Measurement of the error along the *x*- and *y*-axis between the cluster of micro particles and the micro-object, and the micro-object and the target structure
2) Calculation of the angle between the micro-object and the target structure.

Reduction to zero of the above errors should lead to an automated micro assembly operation. Automation of 3D micro assembly would give an extra error for each of the aforementioned tasks. In addition, auto-focussing needs to be incorporated to the magnetic system for the control in 3D space.

REFERENCES

[1] H. Van Brusse, J. Peirs, D. Reynaerts, A. Delchambre, G. Reinhart, N. Roth, M. Weck, E. Zussman, “Assembly of Microsystems,” *CIRP Annals - Manufacturing Technology*, vol. 49, no. 2, pp. 451-472, 2000.

[2] S. Martel, C. C. Tremblay, S. Ngakeng, and G. Langlois, “Controlled manipulation and actuation of micro-objects with magnetotactic bacteria,” *Applied Physics Letters*, vol. 89, no. 23, pp. 1-3, 2006.

[3] S. Floyd, C. Pawashe, and M. Sitti, “Two-dimensional contact and noncontact micromanipulation in liquid using an untethered mobile magnetic microrobot,” *IEEE Transactions on Robotics*, vol. 25, no. 6, pp. 1332-1342, December 2009.

[4] C. Pawashe, S. Floyd, E. Diller, and M. Sitti, “Two-dimensional autonomous microparticle manipulation strategies for magnetic microrobots in fluidic environments,” *IEEE Transactions on Robotics*, vol. 28, no. 2, pp. 467-477, April 2012.

[5] P. Valdastri, E. Sinibaldi, S. Caccavaro, G. Tortora, A. Menciassi, and P. Dario, “A Novel Magnetic Actuation System for Miniature Swimming Robots,” *IEEE Transactions on Robotics*, vol. 27, no. 4, pp. 769-779, August 2011.

[6] D. H. Kim, P. S. S. Kim, A. A. Julius, and M. J. Kim, “Three-dimensional control of engineered motile cellular microrobots,” in *Proceedings of the IEEE International Conference on Robotics and Automation (ICRA)*, pp. 721-726, Minnesota, USA, May 2012.

[7] M. P. Kummer, J. J. Abbott, B. E. Kartochvil, R. Borer, A. Sengul, and B. J. Nelson, “OctoMag: an electromagnetic system for 5-DOF wireless micromanipulation,” *IEEE Transactions on Robotics*, vol. 26, no. 6, pp. 1006-1017, December 2010.

[8] S. Martel, O. Felfoul, J.-B. Mathieu, A. Chanu, S. Tamaz, M. Mohammadi, M. Mankiewicz, and N. Tabatabaei , “MRI-based medical nanorobotic platform for the control of magnetic nanoparticles and flagellated bacteria for target interventions in human capillaries,” *The International Journal of Robotics Research*, vol. 28, no. 9, pp. 1169-1182, September 2009.

[9] S. Martel and M. Mohammadi, “Towards mass-scale micro-asssembly systems using magnetotactic bacteria,” *International Manufacturing Science and Engineering Conference (ASME)*, vol. 2, no. 6, pp. 487-492, Oregon, USA, June 2011.

[10] S. Martel and M. Mohammadi, “Using a swarm of self-propelled natural microrobots in the form of flagellated bacteria to perform complex micro-assembly tasks,” in *Proceedings of The IEEE International Conference on Robotics and Automation*, pp. 500-505, Alaska, USA, May 2010.

[11] S. Fatikow, “Microrobots Take On Microassembly Tasks, ”*mst news*, vol. 22, pp. 20-26, 1997.

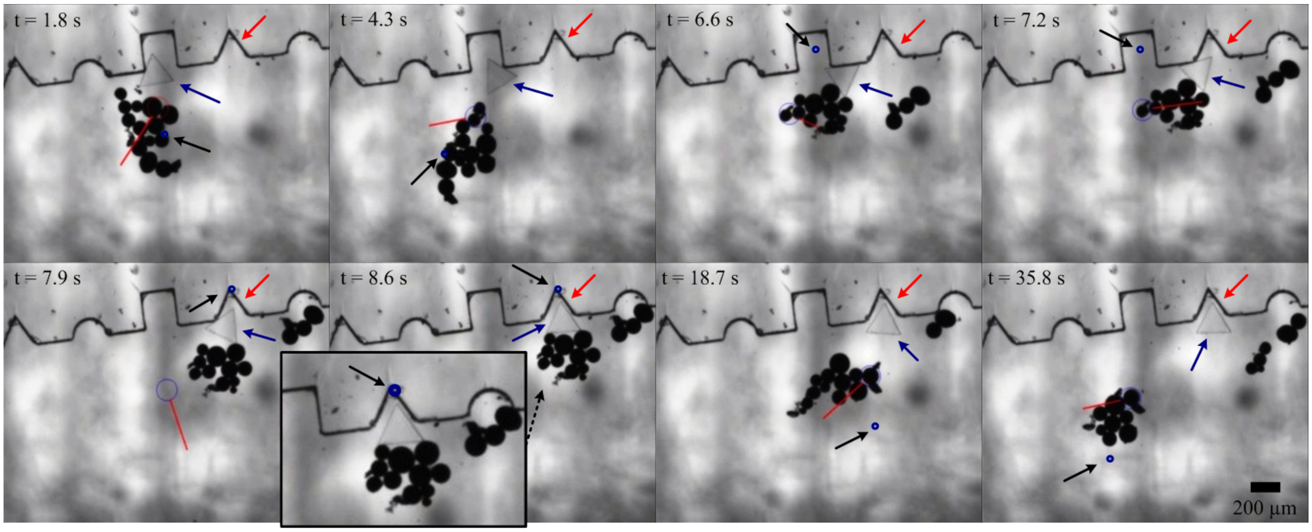

Fig. 16. Microassembly of a triangular microobject to a micro-structure using a cluster of micro particles at various time (t) instants. The cluster selectively steers the micro-object towards the triangular destination within the micro-object. The cluster pulls and pushes the micro-object under the influence of the magnetic fields generated by the control law (34). The execution time of this micro assembly operation is 18 s. During this micro assembly experiment, the average velocity of the cluster is 204 μm/s, and the maximum position tracking error is 50 μm. The controller gains are: $k_{\mathrm{p1}} = k_{\mathrm{p2}} = 10$ s^{-2}, $k_{\mathrm{d1}} = k_{\mathrm{d2}} = 20$ s^{-1} and $g = 30$ rad/s. The large blue (light) circle is assigned by our feature tracking software [28], whereas the small blue circle indicates the reference position. The red line indicates the velocity vector of the cluster of micro particles. The black arrows indicate the triangular destination within the micro-structure, whereas the blue arrows indicate the micro-object. The micro-object has an edge length of 190 μm. Paramagnetic micro particles with average diameter of 100 μm are used in this experiment (PLAParticles-M-redF-plain from Micromod Partikeltechnologie GmbH, Rostock-Warnemuende, Germany).

[12] S. Fatikow, “Microrobot-Based Assembly of Microsystems, ”*NEXUS Research News*, vol. 1, pp. 12-14, 1998.

[13] B. J. Nelson, I. K. Kaliakatsos, and J. J. Abbott, “Microrobots for minimally invasive medicine,” *The Annual Review of Biomedical Engineering*, vol. 12, pp. 55-85, April 2010.

[14] T. H. Boyer,“ The force on a magnetic dipole,”*American Journal of Physics*,vol. 56, no. 8, pp. 688,August 1988

[15] I. S. M. Khalil, J. D. Keuning, L. Abelmann, and S. Misra, “Wireless magnetic-based control of paramagnetic microparticles,” in *Proceedings of the IEEE RAS/EMBS International Conference on Biomedical Robotics and Biomechatronics (BioRob)*, pp. 460-466, Rome, Italy, June 2012.

[16] H. C. Berg, Random Walks in Biology, *Princeton University Press*,1933.

[17] I. S. M. Khalil, R. M. P. Metz, L. Abelmann, and S. Misra, “Interaction force estimation during manipulation of microparticles,” in *Proceedings of the IEEE International Conference of Robotics and Systems (IROS)*, Vilamoura, Portugal, pp. 950-956, October 2012

[18] M. Savia and H.N.Koivo, “Contact Micromanipulation-Survey of Strategies, ”*IEEE/ASME Transactions on Mechatronics*, vol. 14, no. 4, pp. 504-514, August 2009.

[19] M. S. Sakar, E. B. Steager, D. H. Kim, A. A. Julius, M. Kim, V. Kumar and G. J. Pappas, “Modeling, control and experimental characterization of microbiorobots,” *The International Journal of Robotics Research*, vol. 30, no. 6, pp. 647-658, May 2011.

[20] Z. Lu and S. Martel, “Controlled bio-carriers based on magnetotactic bacteria,” in *Proceedings of The IEEE International Conference on Solid-State Sensors, Actuators and Microsystems*, pp. 683-686, Lyon, France, June 2007.

[21] Z. Lu and S. Martel, ”Preliminary investigation of bio-carriers using magnetotactic bacteria,” in *Proceedings of The IEEE Engineering in Medicine and Biology Society Annual International Conference (EMBS)*, pp. 683-686, New York City, USA, September 2006.

[22] S. S. Shevkoplyas, A. C. Siegel, R. M. Westervelt, M. G. Prentiss, and G. M. Whitesides, “The force acting on a superparamagnetic bead due to an applied magnetic field,” *Lab on a Chip*, vol. 7, no. 10, pp. 1294-1302, July 2007.

[23] S. Komada, N. Machii, and T. Hori, “Control of redundant manipulators considering order of disturbance observer,” *IEEE Transactions on Industrial Electronics*, vol. 47, no. 2, pp. 413-420, April 2000.

[24] S. Katsura, Y. Matsumoto, and K. Ohnishi, “Modeling of force sensing and validation of disturbance observer for force control,” *IEEE Transactions on Industrial Electronics*, vol. 54, no. 1, pp. 530-538, February 2007.

[25] B. E. Kratochvil, M. P. Kummer, S. Erni, R. Borer, D. R. Frutiger, S. Schurle, and B. J. Nelson, “MiniMag: a hemispherical electromagnetic system for 5-DOF wireless micromanipulation,” in *Proceedings of the 12th International Symposium on Experimental Robotics-Springer Tracts in Advanced Robotics*, New Delhi, India, December 2010.

[26] R. G. McNeil, R. C. Ritter, B. Wang, M. A. Lawson, G. T. Gillies, K. G. Wika, E. G. Quate, M. A. Howard, and M. S. Grady, “Characteristics of an improved magnetic-implant guidance system,” *IEEE Transactions on Biomedical Engineering*, vol. 42, no. 8, pp. 802-808, August 1995.

[27] I. S. M. Khalil, M. P. Pichel, L. Zondervan, L. Abelmann, and S. Misra, “Characterization and control of biological microrobots,” in *Proceedings of the 13th International Symposium on Experimental Robotics-Springer Tracts in Advanced Robotics*, Quebec City, Canada, June 2012.

[28] J. D. Keuning, J. de Vries, L. Abelmann, and S. Misra, “Image-based magnetic control of paramagnetic microparticles in water,” in *Proceedings of the IEEE International Conference of Robotics and Systems (IROS)*, pp. 421-426, San Francisco, USA, September 2011.

[29] B. Shapiro, Ed. (2008, Nov. 20). Control and system integration of micro- and nanoscale systems. NSF Workshap Report, March 29-30, 2004

Appendix

UNIVERSITY OF TWENTE.

MODELING AND MAGNETIC-BASED MOTION CONTROL OF A CLUSTER OF MICROPARTICLES

FRANK VAN DEN BRINK

INTRODUCTION

CONTROL OF MICRO PARTICLES

- Control of single micro particles
- To provide greater magnetic force: a cluster is used

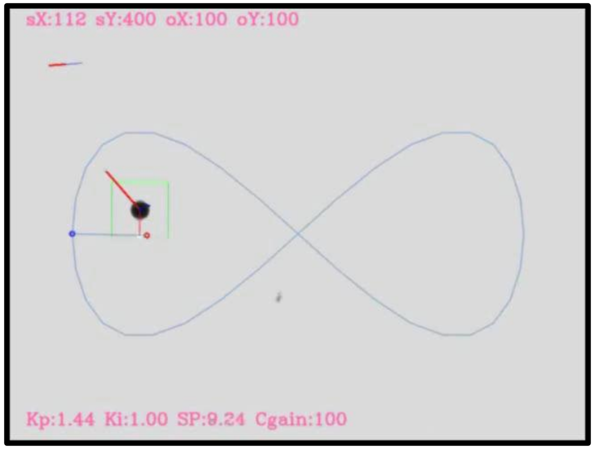

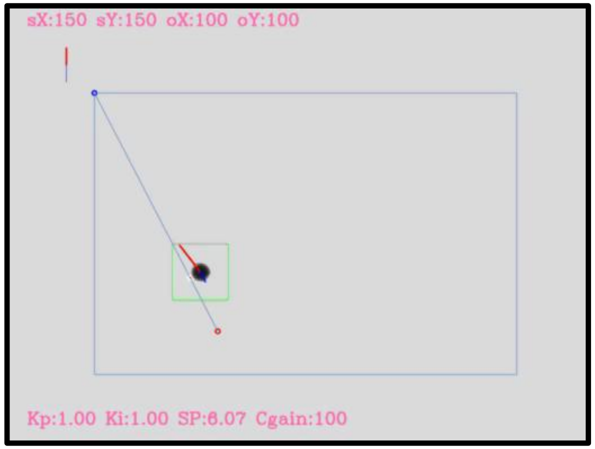

INTRODUCTION
APPLICATIONS

- Minimally invasive surgery (MIS)

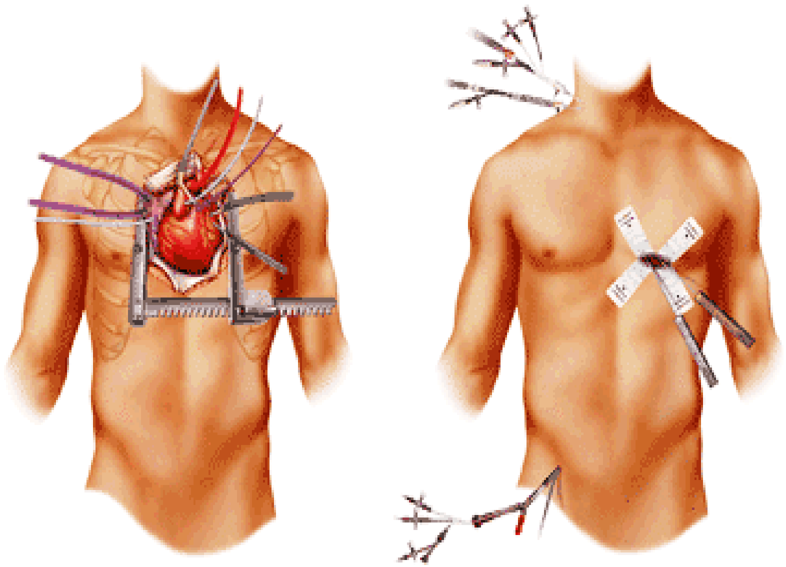

Open heart surgery vs. MIS
Picture courtesy: Anova Heart and Vascular Institute

Da Vinci Surgical System

INTRODUCTION
APPLICATIONS

- Micro assembly for Micro Electromechanical Systems (MEMS)

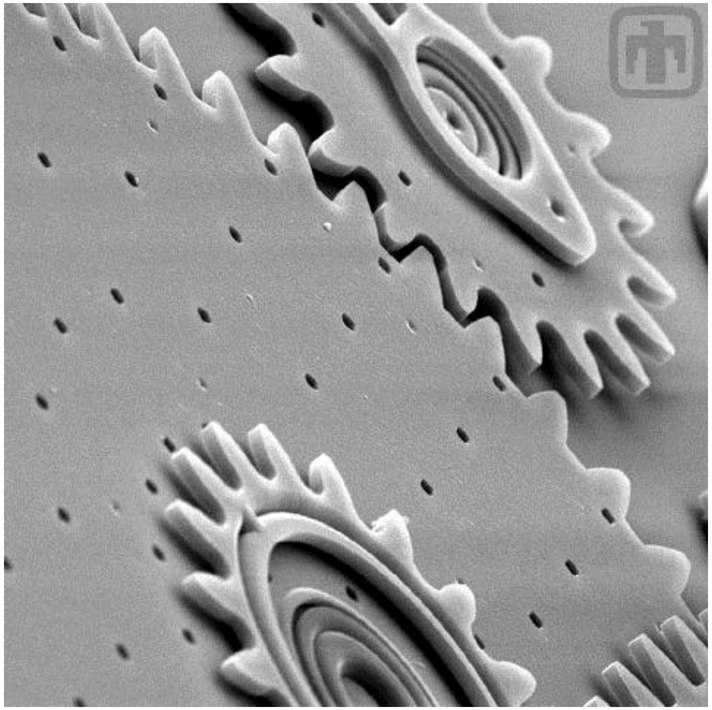

Sandia National Laboratories

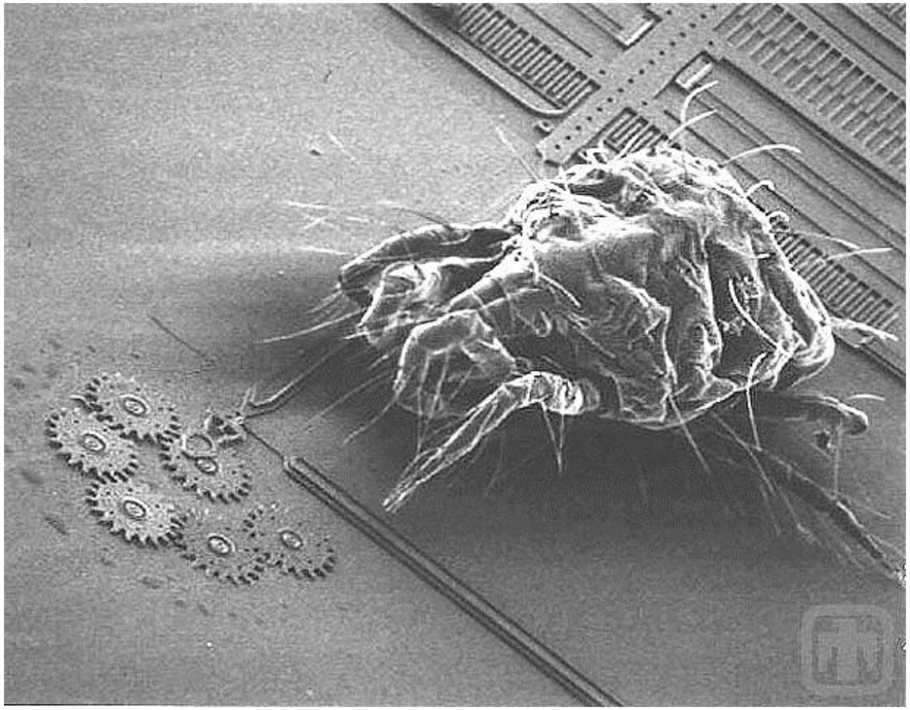

Sandia National Laboratories

INTRODUCTION
RELATED WORK

- Wireless magnetic-based manipulation
- Wireless micro assembly

Octomag (M.P. Kummer *et al.,* 2010)

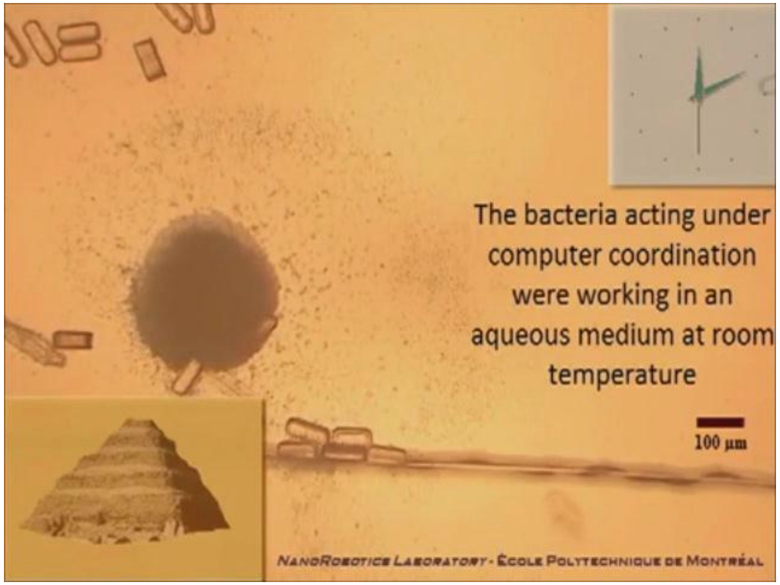

Magnetic bacteria (S. Martel *et al., 2010)*

INTRODUCTION
APPROACH

- Optimal cluster size
- Closed loop control
- Micro manipulation
- Micro assembly application

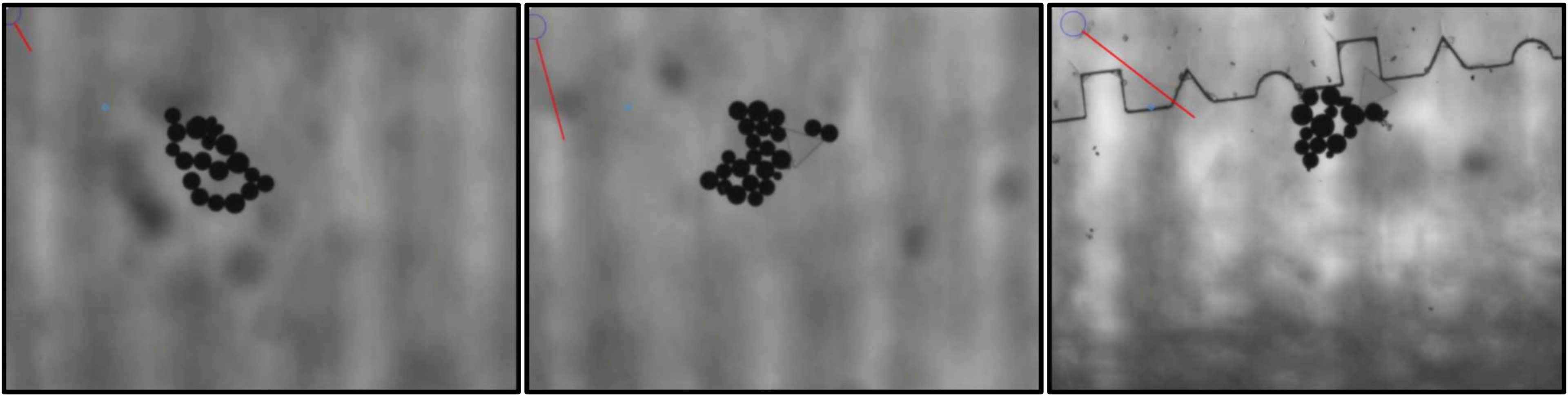

MODELING AND CONTROL
MAGNETIC SYSTEM

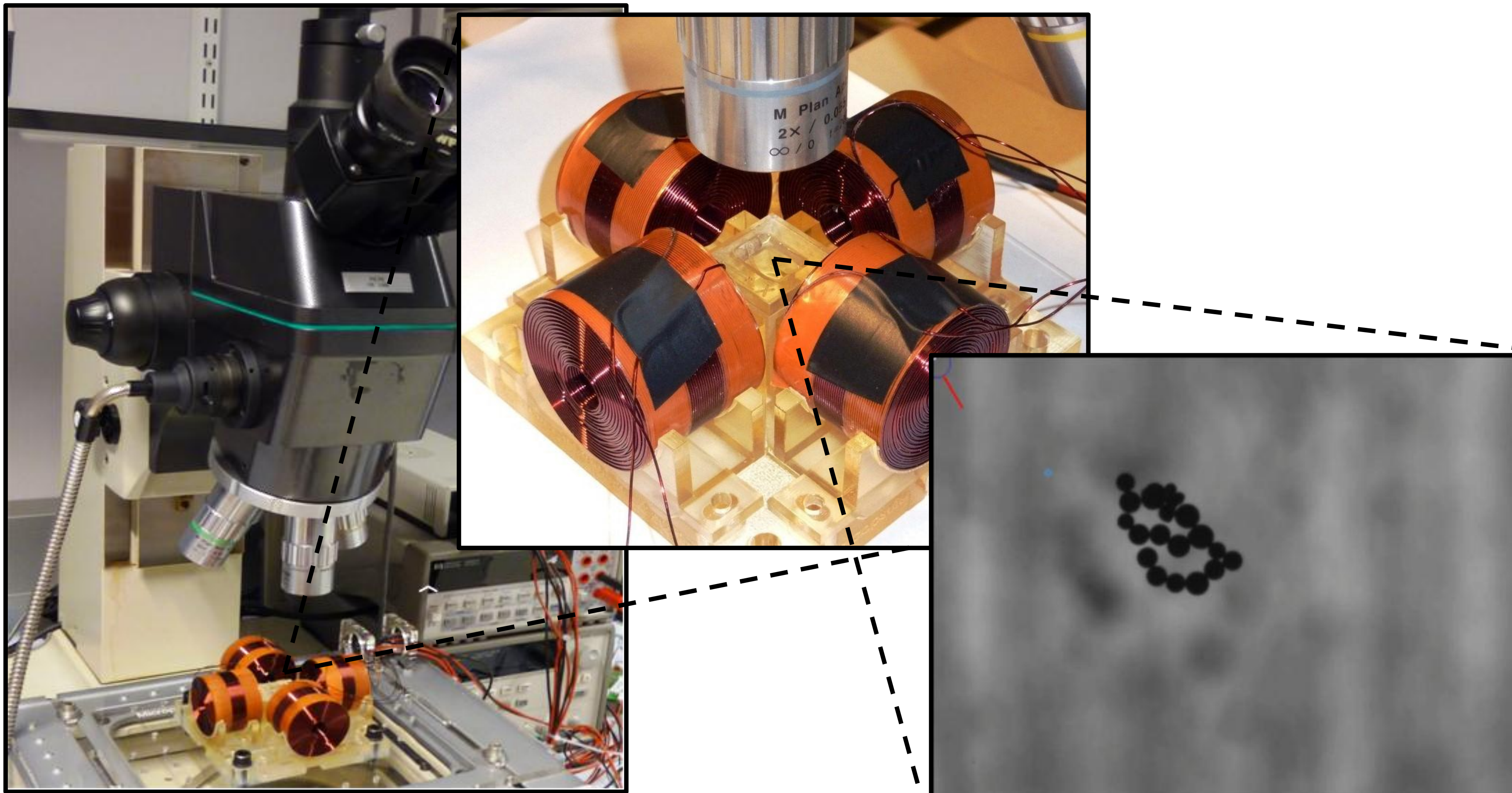

MODELING AND CONTROL
MODELING

$\mathbf{F}(\mathbf{P})$: Magnetic force

$\mathbf{F}_{\mathrm{dc}}$: Drag force on the cluster

$\mathbf{F}_{\mathrm{do}}$: Drag force on micro-object

M : Mass of the cluster

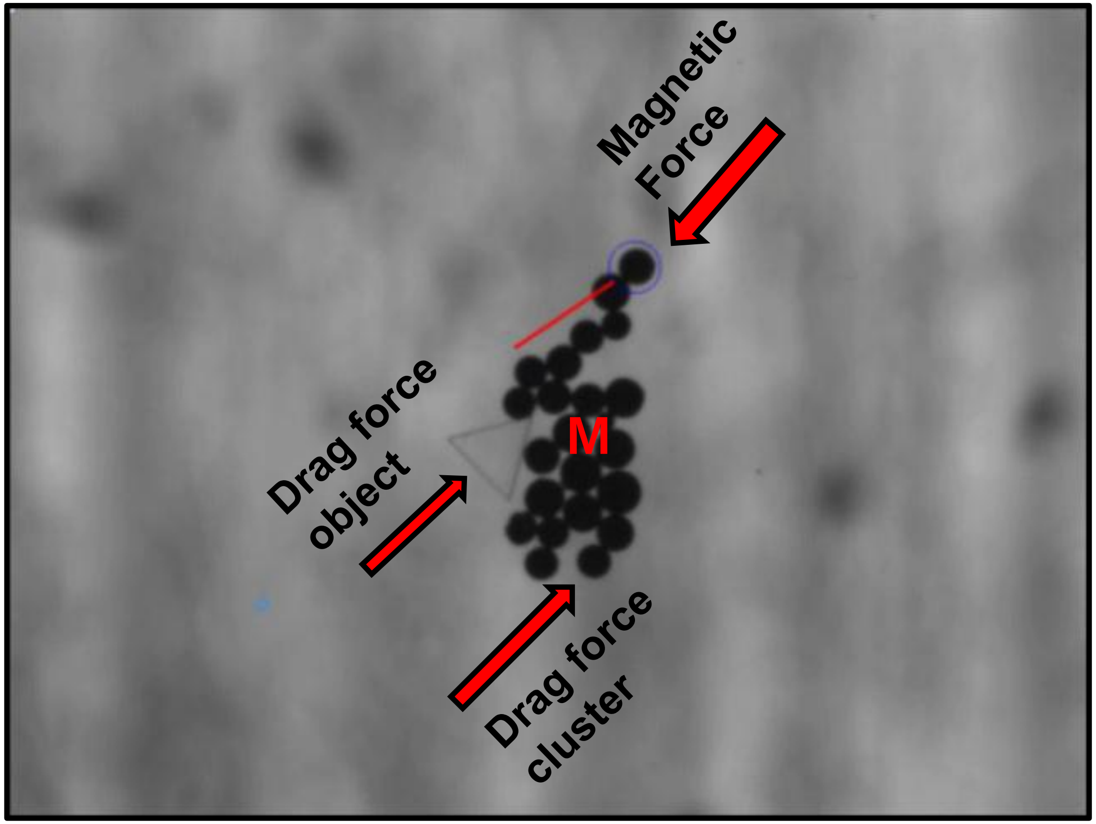

MODELING AND CONTROL
EQUATION OF MOTION

R_e > 0.1 → $\mathbf{F}(\mathbf{P}) - \mathbf{F}_{\mathrm{dc}}(\dot{\mathbf{P}}) - \mathbf{F}_{\mathrm{do}}(\dot{\mathbf{P}}) = \mathrm{M}\ddot{\mathbf{P}}$

R_e < 0.1 → $\mathbf{F}(\mathbf{P}) - \mathbf{F}_{\mathrm{dc}}(\dot{\mathbf{P}}) - \mathbf{F}_{\mathrm{do}}(\dot{\mathbf{P}}) = 0$

$\mathbf{F}(\mathbf{P})$: Magnetic force

$\mathbf{F}_{\mathrm{do}}$: Drag force on micro-object

$\mathbf{F}_{\mathrm{dc}}$: Drag force on the cluster

M : Mass of the cluster

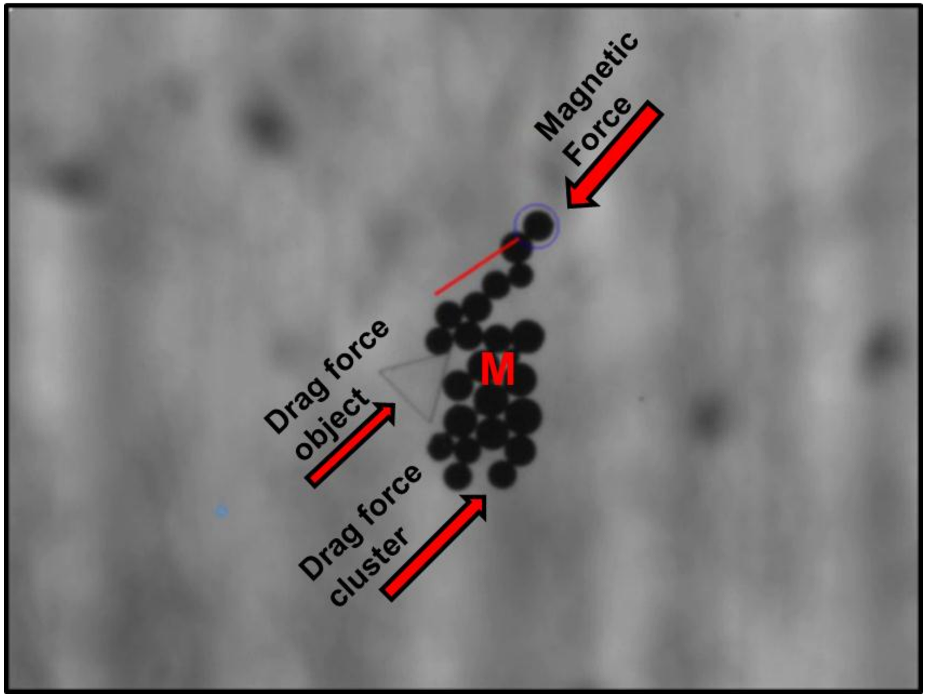

MODELING AND CONTROL
MAGNETIC FORCE MODELING

Magnetic force: $$\mathbf{F}(\mathbf{P}) = \nabla\left(\mathbf{m}(\mathbf{P})\cdot\mathbf{B}(\mathbf{P})\right) = \frac{4}{3}\frac{1}{\mu}\pi r_p^3 \chi_m \nabla\left(\mathbf{B}^2(\mathbf{P})\right) \quad (1)$$

Magnetic field: $$\mathbf{B}_e(\mathbf{P}) = \widetilde{\mathbf{B}}_e(\mathbf{P}) i_e \quad (2)$$

$$\mathbf{B}(\mathbf{P}) = \sum_{e=1}^{m} \mathbf{B}_e(\mathbf{P}) = \sum_{e=1}^{m} \widetilde{\mathbf{B}}_e(\mathbf{P}) i_e \quad (3)$$

$\mathbf{m}(\mathbf{P})$: Magnetic dipole moment

$\widetilde{\mathbf{B}}_e(\mathbf{P})$: Magnetic field map

$\mathbf{I}$: current vector

$\mathbf{B}(\mathbf{P})$: Magnetic field

i_e : Current through the e_{th} electromagnet

μ : Permeability coefficient

χ_m : Magnetic susceptibility

r_p : Micro particle radius

$$\boxed{\begin{aligned} \mathbf{F}(\mathbf{P}) &= \alpha_{\mathrm{p}}\frac{4}{3}\pi r_{\mathrm{p}}^3 \mathbf{I}^{\mathrm{T}} \nabla(\widetilde{\mathbf{B}}^{\mathrm{T}}(\mathbf{P})\widetilde{\mathbf{B}}(\mathbf{P}))\mathbf{I} \quad (4) \\ \mathbf{F}_{\mathrm{c}}(\mathbf{P}) &= \sum_{i=1}^{n} \alpha_{\mathrm{p}}\frac{4}{3}\pi r_{\mathrm{pi}}^3 \mathbf{I}^{\mathrm{T}} \nabla(\widetilde{\mathbf{B}}^{\mathrm{T}}(\mathbf{P})\widetilde{\mathbf{B}}(\mathbf{P}))\mathbf{I} \quad (5) \end{aligned}}$$

MODELING AND CONTROL
DRAG FORCE MODELING AND REYNOLDS NUMBER

Drag force micro particle: $\mathbf{F}_{\mathrm{d}}(\dot{\mathbf{P}}) = F_{\mathrm{p}}\eta\dot{\mathbf{P}}$ $\quad \mathbf{F}_{\mathrm{d}}(\dot{\mathbf{P}}) = 6\pi\eta r_{\mathrm{p}}\dot{\mathbf{P}}$

Drag force cluster: (Disc) $\mathbf{F}_{\mathrm{dc}}(\dot{\mathbf{P}}) = F_{\mathrm{c}}\eta\dot{\mathbf{P}}$ $\quad \mathbf{F}_{\mathrm{dc}}(\dot{\mathbf{P}}) = \frac{32\sqrt{n}\ r_{\mathrm{p}}}{3}\eta\dot{\mathbf{P}}$

Reynolds number micro particle: $R_e = \Omega_{\mathrm{p}}\frac{\rho_{\mathrm{f}}v}{\eta}$ $\quad R_e = \frac{2\rho_{\mathrm{f}}v r_{\mathrm{p}}}{\eta}$

Reynolds number cluster: $R_{ec} = \Omega_{\mathrm{c}}\frac{\rho_{\mathrm{f}}v}{\eta}$ $\quad \boxed{R_{ec} = \frac{32\sqrt{n}r_{\mathrm{p}}\rho_{\mathrm{f}}v}{9\pi\eta}}$

$$\frac{F_{\mathrm{p}}}{\Omega_{\mathrm{p}}} = \frac{F_{\mathrm{c}}}{\Omega_{\mathrm{c}}}$$

F_{p} : Drag shape factor micro particle

F_{c} : Drag shape factor cluster

Ω_{p} : Reynolds shape factor micro particle

Ω_{c} : Reynolds shape factor cluster

η : Fluid dynamic viscosity

ρ_{f} : Fluid density

MODELING AND CONTROL
OPTIMAL CLUSTERSIZE

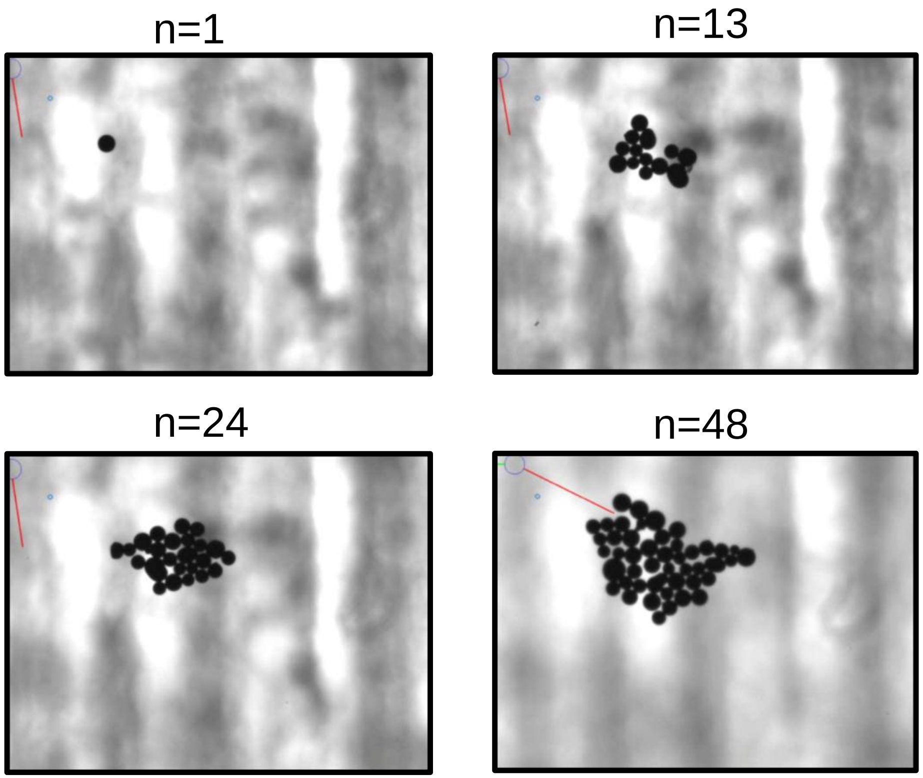

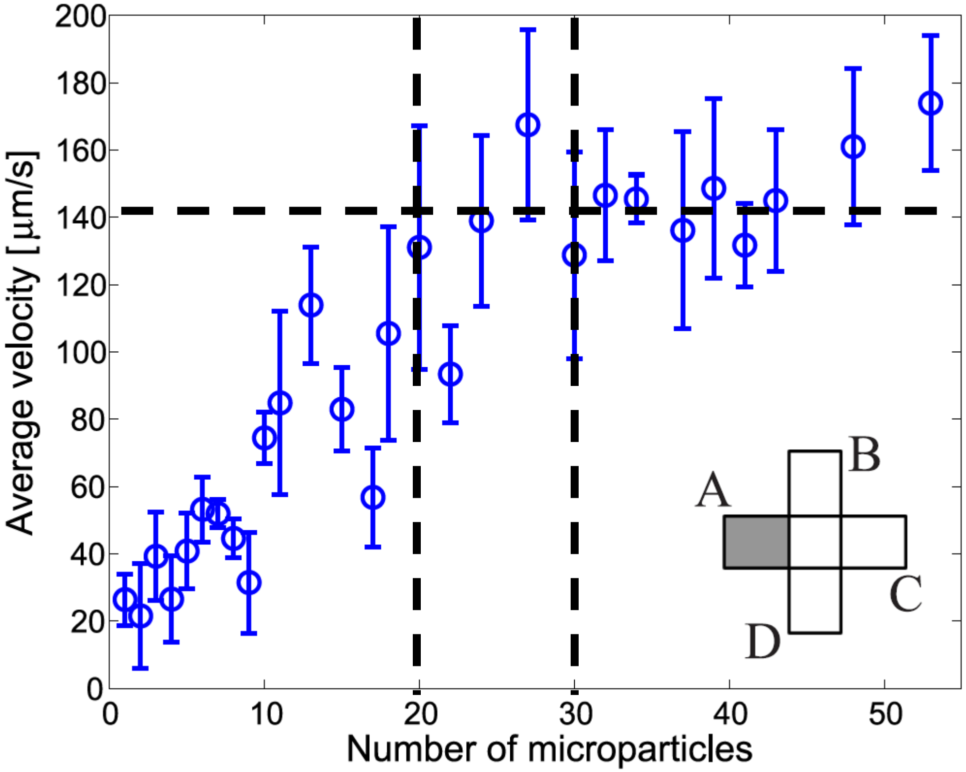

Assymptote at ~140 µm/s and 20 micro particles

MODELING AND CONTROL

EQUATION OF MOTION

$$\boxed{R_{ec} = \frac{32\sqrt{n} r_{\mathrm{p}} \rho_{\mathrm{f}} v}{9\pi\eta}}$$

$$\boxed{R_e} \rightarrow < 0.1 \rightarrow \mathbf{F}(\mathbf{P}) - \mathbf{F}_{\mathrm{dc}}(\dot{\mathbf{P}}) - \mathbf{F}_{\mathrm{do}}(\dot{\mathbf{P}}) = 0$$

Velocity range of 200 µm/s to 500 µm/s
Particles 70% to 100% submerged

$$0.0353 < R_e < 0.1260$$

$$\mathbf{F}_{\mathrm{dc}}(\dot{\mathbf{P}}) = \frac{32\sqrt{n}\ r_{\mathrm{p}}}{3}\eta\dot{\mathbf{P}}$$

$$\boxed{\mathbf{F}(\mathbf{P}) - \mathbf{F}_{\mathrm{dc}}(\dot{\mathbf{P}}) - \mathbf{F}_{\mathrm{do}}(\dot{\mathbf{P}}) = 0}$$

$$\mathbf{F}_{\mathrm{c}}(\mathbf{P}) = \sum_{i=1}^{n} \alpha_{\mathrm{p}} \frac{4}{3}\pi r_{\mathrm{pi}}^{3} \mathbf{I}^{\mathrm{T}} \nabla(\widetilde{\mathbf{B}}^{\mathrm{T}}(\mathbf{P})\widetilde{\mathbf{B}}(\mathbf{P}))\mathbf{I}$$

MODELING AND CONTROL

MODEL VERIFICATION

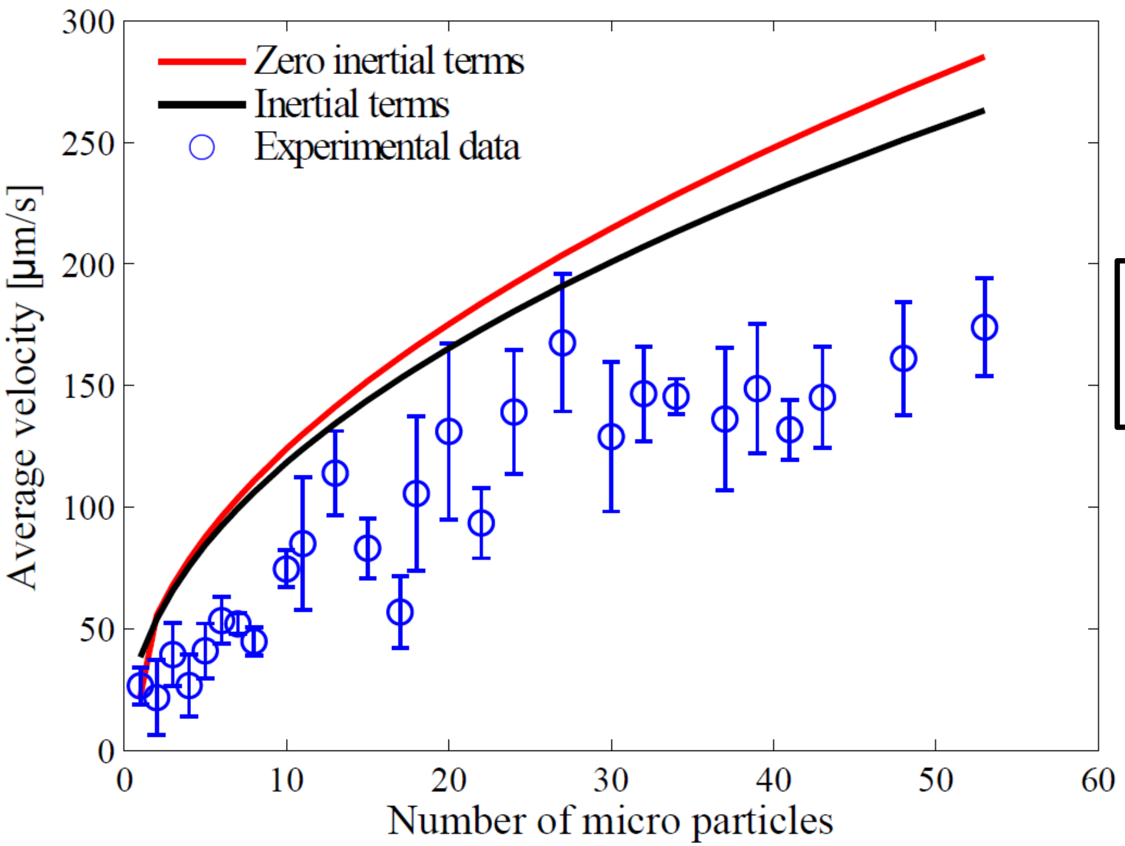

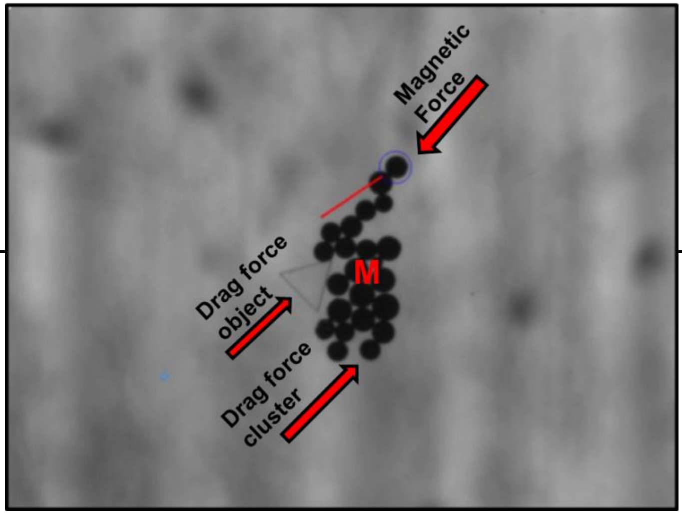

$$\mathbf{F}(\mathbf{P}) - \mathbf{F}_{\mathrm{dc}}(\dot{\mathbf{P}}) - \mathbf{F}_{\mathrm{do}}(\dot{\mathbf{P}}) = 0$$
$$\mathbf{F}(\mathbf{P}) - \mathbf{F}_{\mathrm{dc}}(\dot{\mathbf{P}}) - \mathbf{F}_{\mathrm{do}}(\dot{\mathbf{P}}) = \mathrm{M}\ddot{\mathbf{P}}$$

Inertial term has no significant influence

MODELING AND CONTROL
SHAPE ANALYSIS

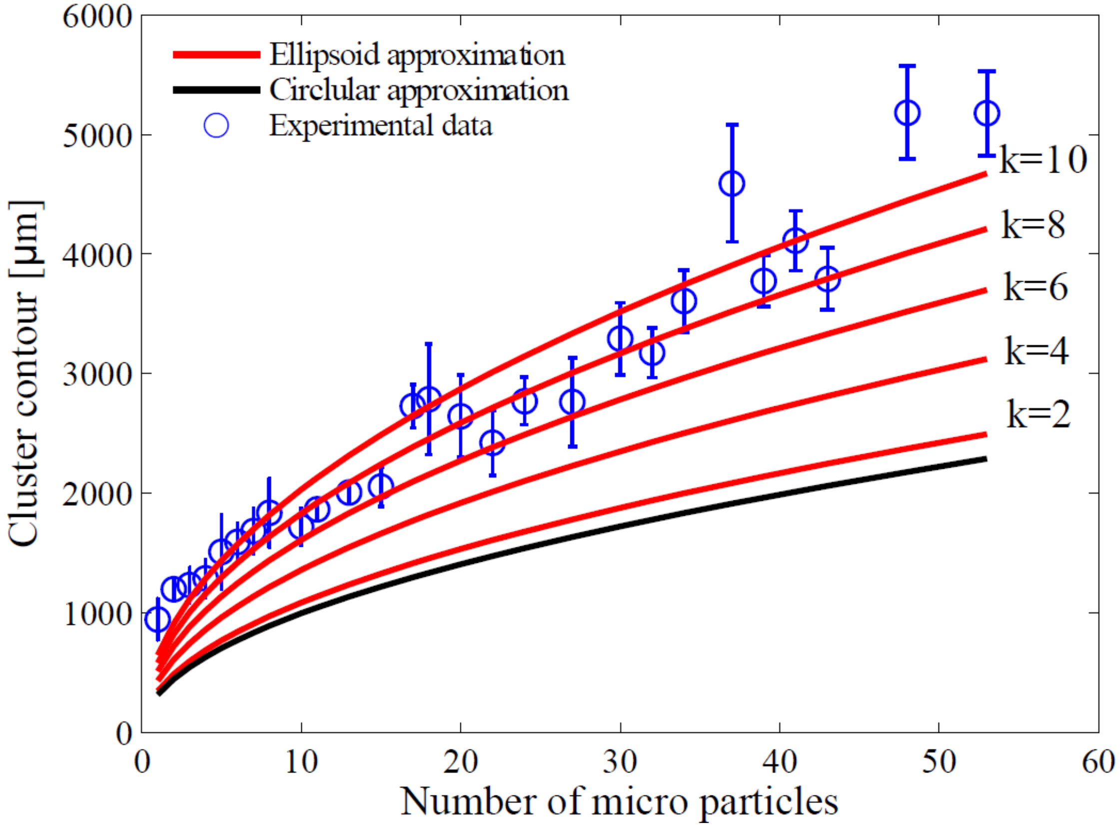

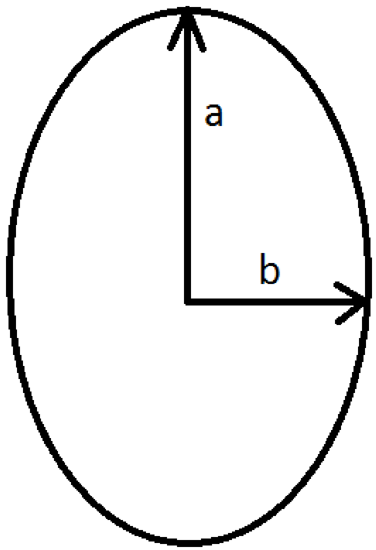

K = ratio a/b

K = 8 gives the best result

MODELING AND CONTROL
SHAPE ANALYSIS

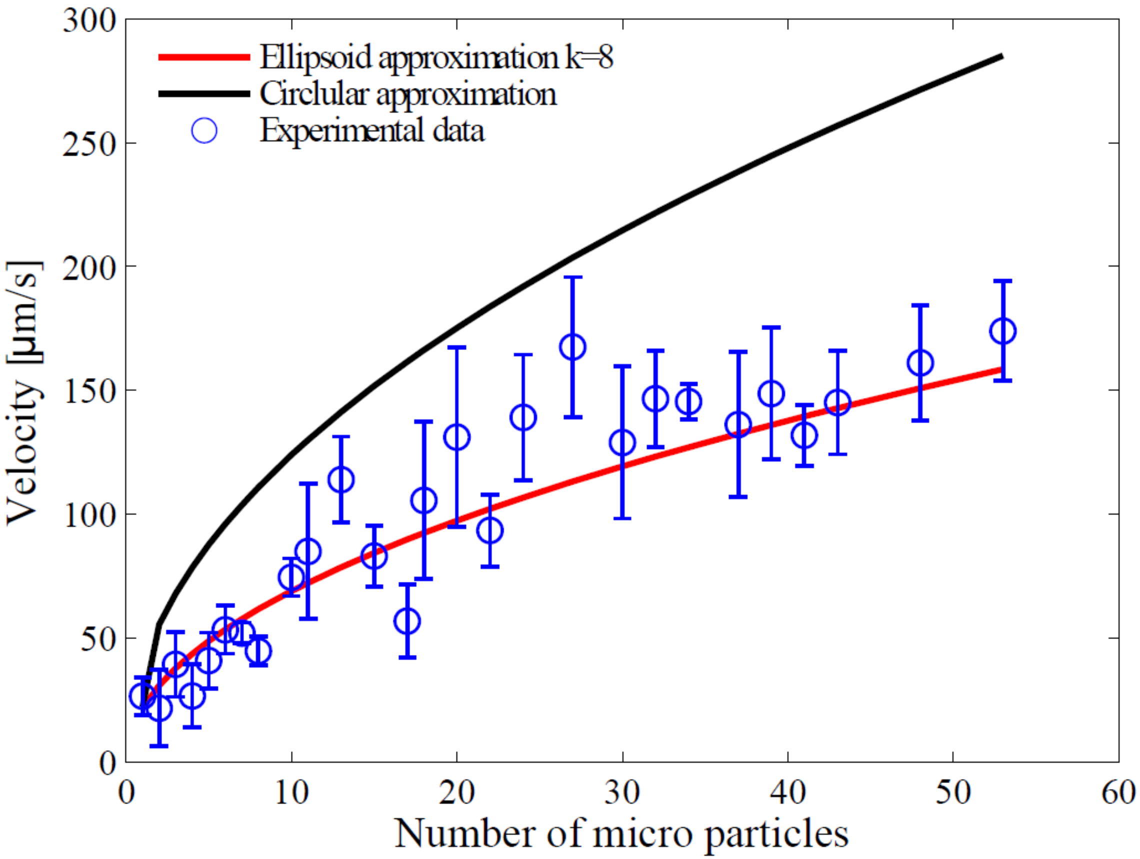

Ellipsoid ratio k = 8

Drag force ellipsoid:

$$\mathbf{F}_{\mathrm{de}}(\dot{\mathbf{P}}) = \frac{6\pi\eta a}{\ln\left(\frac{2a}{b}\right)}\dot{\mathbf{P}}$$

MODELING AND CONTROL
CONTROL

$$\boxed{\mathbf{F}(\mathbf{P}) - \mathbf{F}_{\mathrm{de}}(\dot{\mathbf{P}}) = 0}$$

$$\mathbf{F}(\mathbf{P}) = \widehat{\mathbf{F}}_{\mathrm{d}}(\dot{\mathbf{P}}) - \mathrm{M}_{\mathrm{n}}\left(\mathbf{K}_{\mathbf{d}}\dot{\mathbf{e}} + \mathbf{K}_{\mathbf{p}}\mathbf{e}\right)$$

$$k_d = 20\ s^{-1}, k_p = 10\ s^{-2}$$

$$\widehat{\mathbf{F}}_{\mathrm{d}}(\dot{\mathbf{P}}) \triangleq \widehat{\mathbf{F}}_{\mathrm{dc}}(\dot{\mathbf{P}}) + \widehat{\mathbf{F}}_{\mathrm{do}}(\dot{\mathbf{P}})$$

$$\widehat{\mathbf{F}}_{\mathrm{d}}(\mathbf{P}) = \frac{g}{s+g}\left[\mathbf{F}(\mathbf{P}) - g\mathrm{M}_{\mathrm{n}}\dot{\mathbf{P}}\right] - g\mathrm{M}_{\mathrm{n}}\dot{\mathbf{P}}$$

$$g = 30\ \text{rad/s}$$

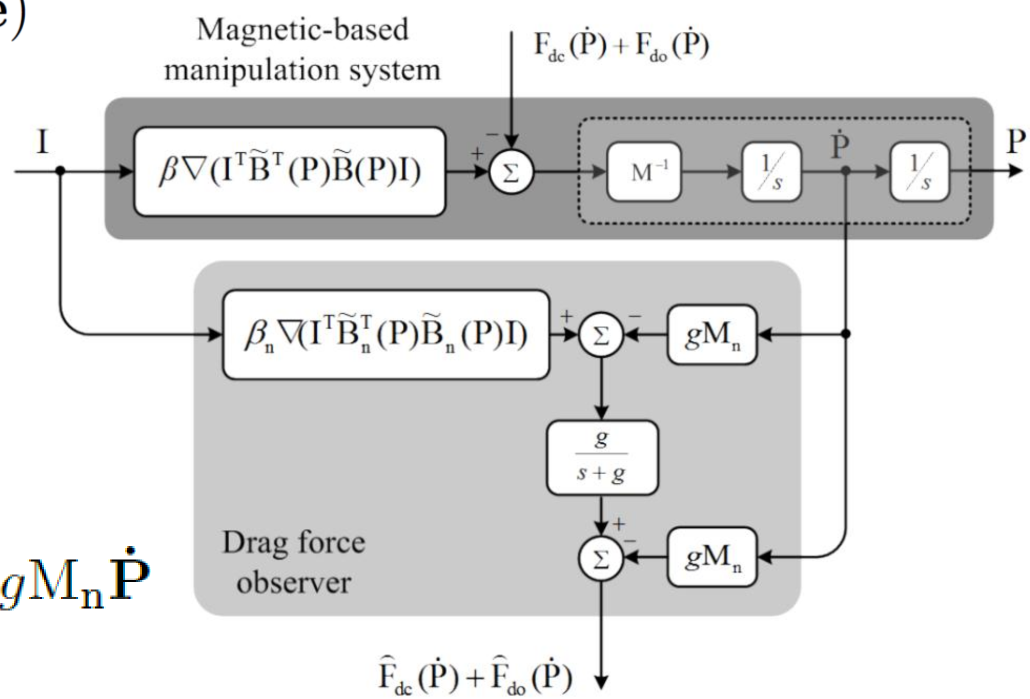

Icra 2013

RESULTS
POINT-TO-POINT CONTROL OF A CLUSTER OF MICRO PARTICLES

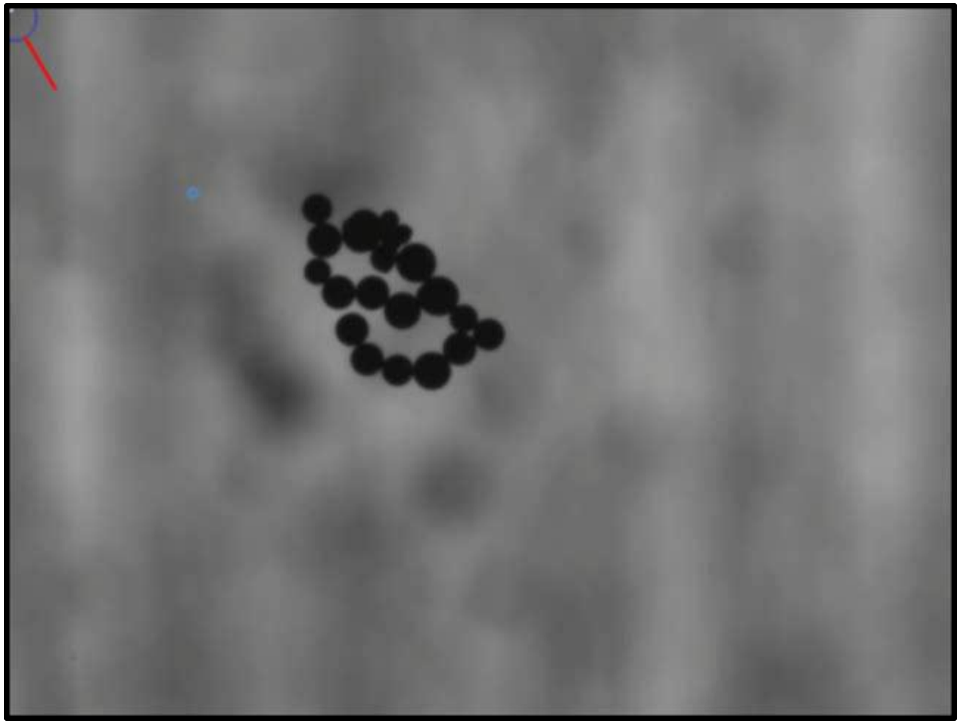

- Maximum average velocity of 327 µm/s
- Maximum average tracking error of 110 µm

RESULTS

MICRO OBJECTS AND TARGETSTRUCTURE

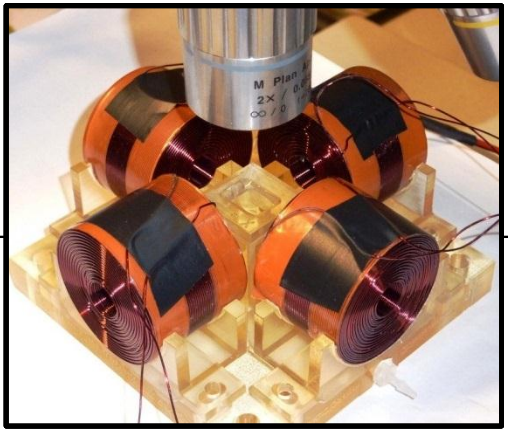

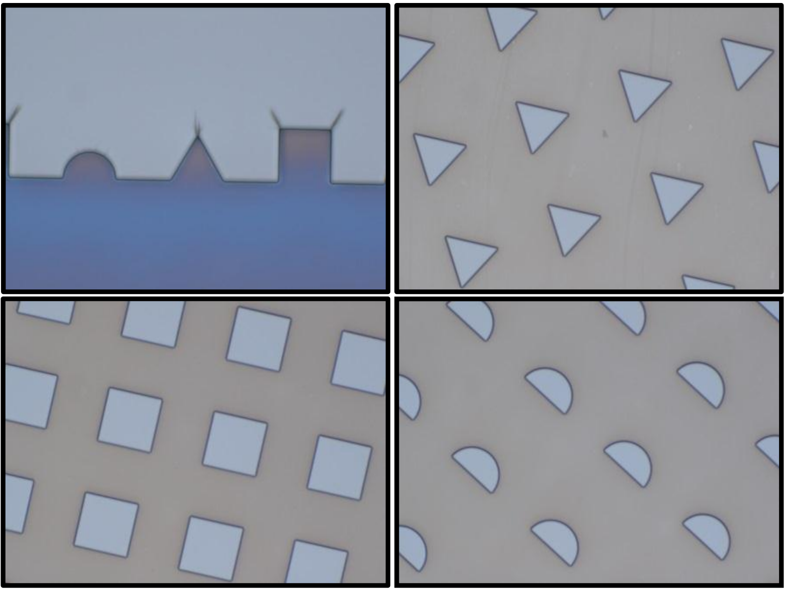

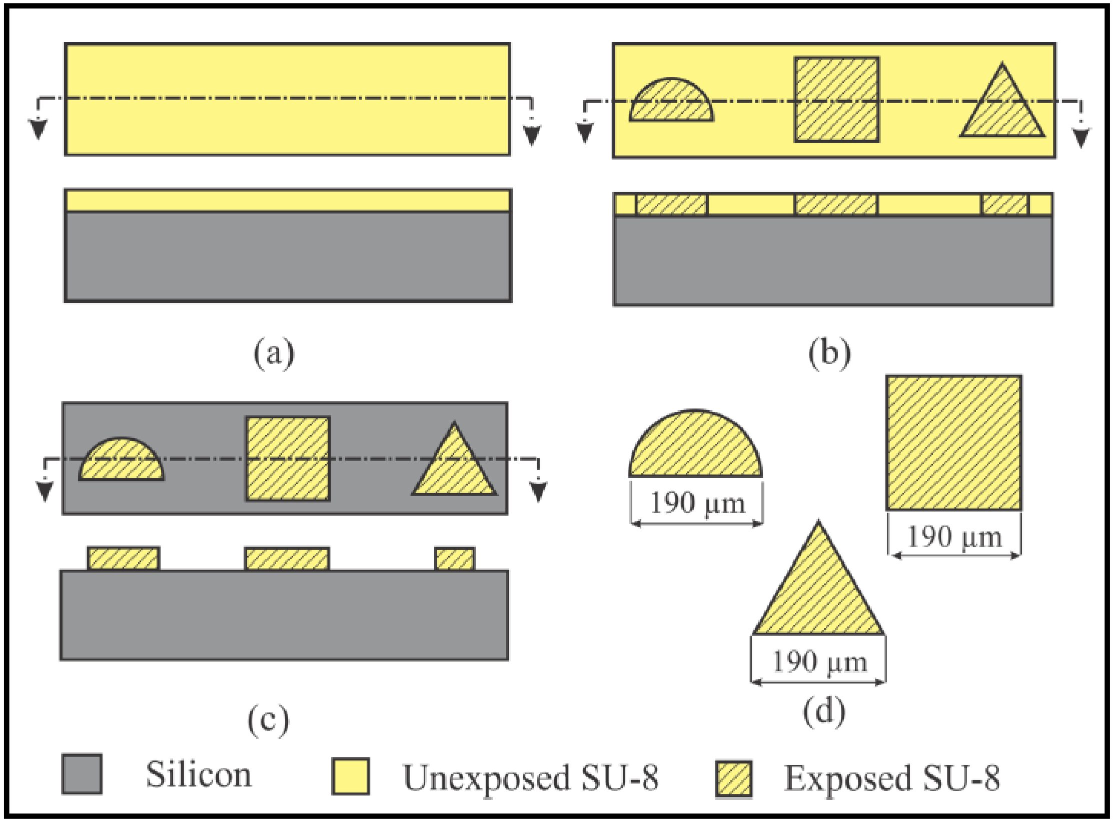

RESULTS

POINT-TO-POINT CONTROL OF A MICRO-OBJECT

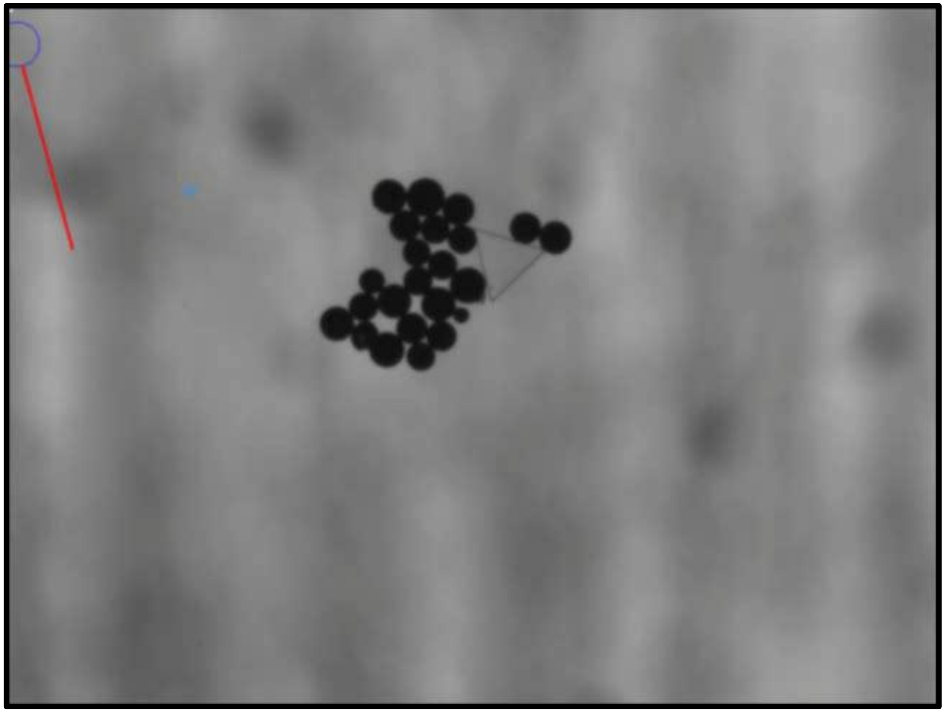

- Maximum average velocity of 297 µm/s
- Maximum average tracking error of 150 µm

RESULTS

MICRO ASSEMBLY APPLICATION

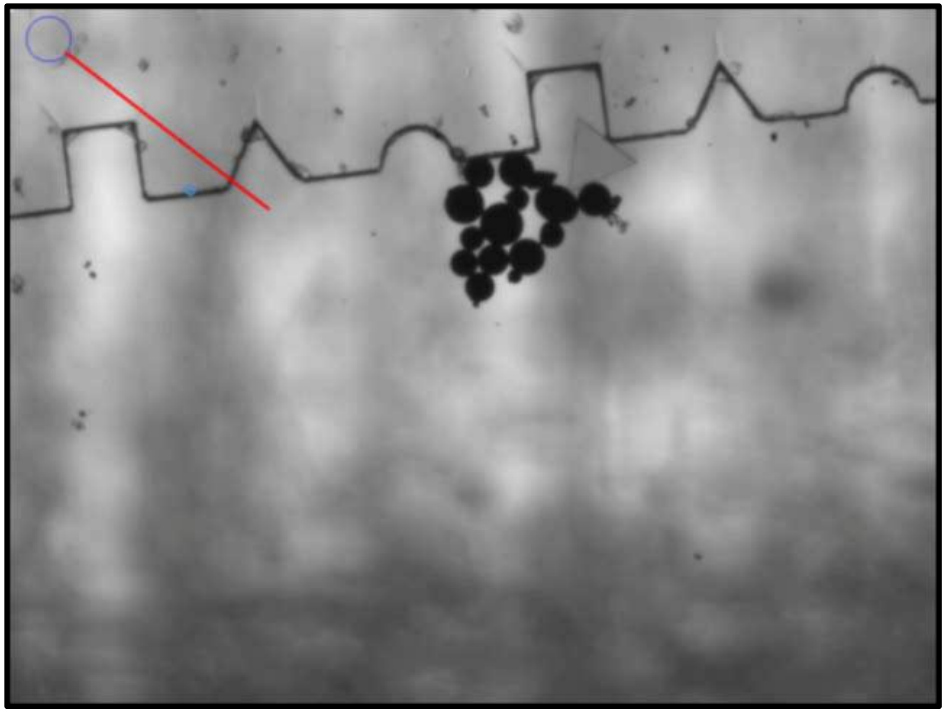

- Proof of concept
- Average velocity of 194 μm/s
- Execution time of 18 s

- Feasible but still a lot to learn about interaction forces

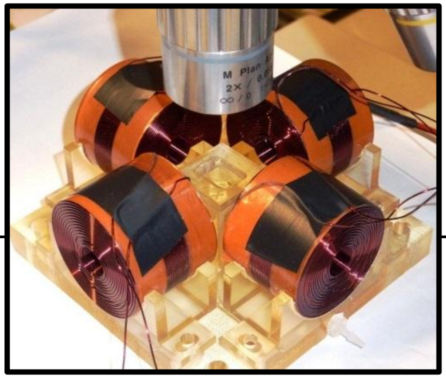

CONCLUSIONS

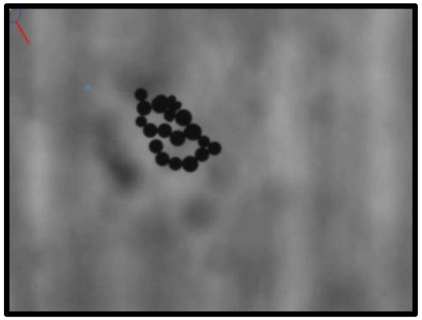

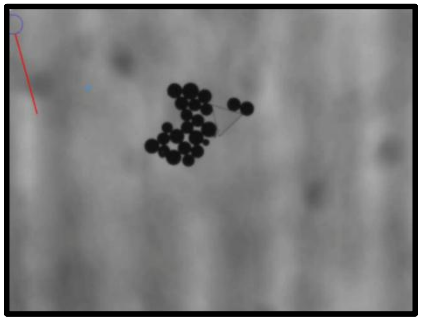

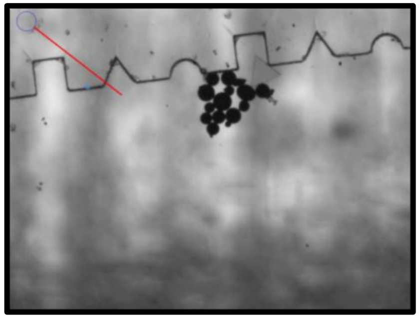

- Optimal cluster size of ~20 microparticles
- Point-to-point control: maximum average velocity 327 µm/s and maximum average tracking error of 110 µm
- Micro manipulation: maximum average velocity 297 µm/s and maximum average tracking error of 150 µm
- Micro assembly with an average velocity of 193 µm/s in 18 s

FUTURE WORK

- Investigation of interaction forces at micro scale
- Control and micro assembly in 3D space
- Automated micro assembly
- Nano scale

CONTRIBUTIONS

I. S. M. Khalil, F. van den Brink, O. S. Sukas, L. Abelmann, and S. Misra, "Microassembly using a cluster of paramagnetic microparticles," in *Proceedings of The IEEE International Conference on Robotics and Automation (ICRA),* Karlsruhe, Germany, May 2013. In Press

THANK YOU

- Questions?